



THE UNIVERSITY OF TENNESSEE

DEPARTMENT OF ELECTRICAL ENGINEERING

A MATHEMATICAL MODEL FOR A SPACE VEHICLE

THRUST VECTOR CONTROL SYSTEM

Z. Thompson and J. C. Hung

Partially supported by
National Aeronautics and Space Administration
through Grant NsG-351

August 24, 1967

Scientific Report No. 15

Control Theory Group

A MATHEMATICAL MODEL FOR A SPACE VEHICLE
THRUST VECTOR CONTROL SYSTEM

by

Z. Thompson and J. C. Hung

Partially supported by
National Aeronautics and Space Administration
through Grant NsG-351

August 24, 1967

Department of Electrical Engineering
The University of Tennessee

ACKNOWLEDGMENT

The research work reported here was partially supported by the National Aeronautics and Space Administration through Grant NsG-351.

This report contains the essence of a thesis submitted to The University of Tennessee by Zack Thompson for the degree of Master of Science.

TABLE OF CONTENTS

CHAPTER	PAGE
I. INTRODUCTION	1
II. TORQUE MOTOR	12
III. SERVO VALVE	19
IV. LOAD AND REFLECTED LOAD DYNAMICS	33
V. DYNAMIC SHAPING NETWORK	43
VI. SUMMARY	51
LIST OF REFERENCES	61
APPENDICES	65
A. EXAMPLE	66
B. ASSUMPTIONS USED	76

LIST OF FIGURES

FIGURE	PAGE
1. Space Booster	2
2. Engine Cluster	4
3. Single Engine Stage	5
4. Torque Motor Armature and Magnets	13
5. Side View of Torque Motor	14
6. Torque Motor Schematic	15
7. Complete Block Diagram of Servo Valve	18
8. Single Stage Flow Valve	20
9. Variable Sharp Edge Orifice	22
10. Servo Valve Flow Curves	23
11. Sharp Edge Orifice Curves	24
12. Four Quadrant Flow Curves	26
13. Linear Flow Curves	27
14. Simplified Block Diagram	29
15. Free Body Diagram of Servo Valve Spool	31
16. Servo Valve Block Diagram	32
17. Actuator and Load	34
18. Amplitude Response of Reflected Load	37
19. Actuator Piston Free Body Diagram	38
20. Actuator Piston Rod Free Body Diagram	39
21. Engine Free Body Diagram	40

FIGURE	PAGE
22. Shaping Network Schematic	44
23. Shaping Network Free Body Diagram	45
24. Frequency Response of Network	50
25. Schematic of Complete T.V.C.	52
26. System Frequency Response	53
27. System Response with Load Changes	55
28. Overall System Response	56
29. Block Diagram for Analog Simulations	57
30. Response of System with Pressure Loop Gain Adjustment	58
31. Analog Runs of System	59
32. System Block Diagram	67
33. Engine Frequency Response	68
34. Root Locus Plot of Open Loop	70
35. Expanded Root Locus Plot of Load Dipole	71
36. Double Block Diagram	72
37. Single Block Diagram	73
38. Actuator Frequency Response	74

CHAPTER I

INTRODUCTION

In order for man to explore the many challenges of outer space, it is necessary for both man and scientific equipment to be transported to the areas of interest. This is possible through the combined efforts and skills of the many engineering and other scientific fields. A large space booster, such as that shown in Figure 1, must contain all the necessary equipment for accurate control and guidance to the predetermined destination. This is by no means a simple requirement and must involve a tremendous amount of complex equipment. The equipment will normally include more than one onboard computer to solve the many equations on a vast number of vehicle parameters, many of which are changing with time.

One of the more important closed loop systems necessary for guiding and controlling the space booster is the thrust vector control (TVC) system. The objective of this subsystem is to position the thrust vector to some commanded position. The thrust vector is the amount of force generated by an engine, or a cluster of engines, for the purpose of lifting the boost vehicle and its pay load to its destination. The thrust of an engine is usually held constant regardless of the gimbal position. The engines are mounted to the vehicle stage through a gimbal bearing which is designed to have the engine thrust pivot about the center of the bearing. If the geometric center line of the engine is varied

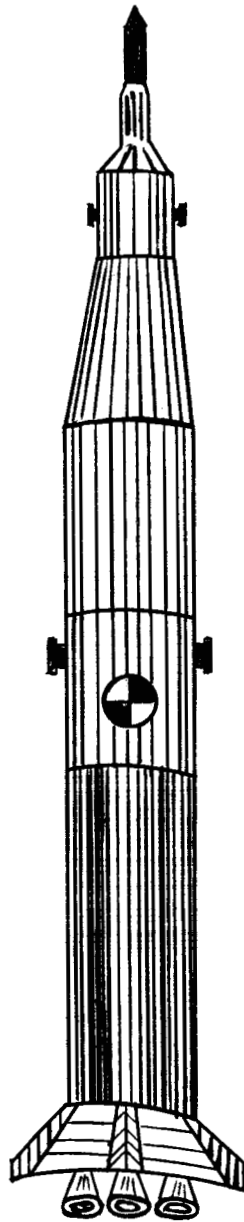


Figure 1. Space booster.

about this gimbal center, it will move with it the actual thrust vector of the engine. It can be seen from Figure 1 that a force at the aft part of the vehicle can produce a large turning moment about the center of mass of the vehicle. This moment is used to determine the angular position of the vehicle and thereby fixing its attitude.

Most space boosters have more than one stage since it is convenient to discard the dead weight of the fuel tanks when they have been depleted. Some of these stages may have a cluster of engines while others may require only one. A cluster of engines might be arranged in a pattern such as that in Figure 2. There may be one or more engines fixed in the center position, which are usually not gimballed for thrust vector control. The engines that are used to change the direction of the resultant thrust vector have two actuators per engine mounted at 90 degrees to each other. These actuators are positioned by a command from the control computer which has scaled the individual signals so that the vehicle can be controlled in pitch, yaw, and roll.

The design of a thrust vector control system must be started early in a vehicle program. It can be seen in Figure 3 and will be more obvious later that many essential parameters of the TVC come from other parts of the stage. The attach points and the spring rate K_v of the vehicle stage structure can affect the stability of the TVC system. As a general rule the stage structure and the engine is not designed from constraints of the TVC system. The control engineer is faced with accepting what he can get and making the system perform regardless of the parameters

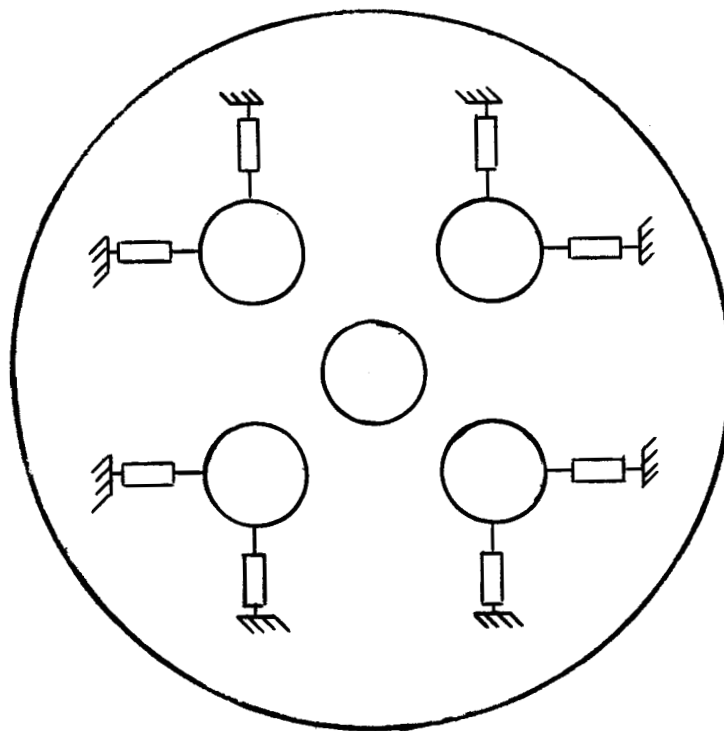


Figure 2. Engine cluster.

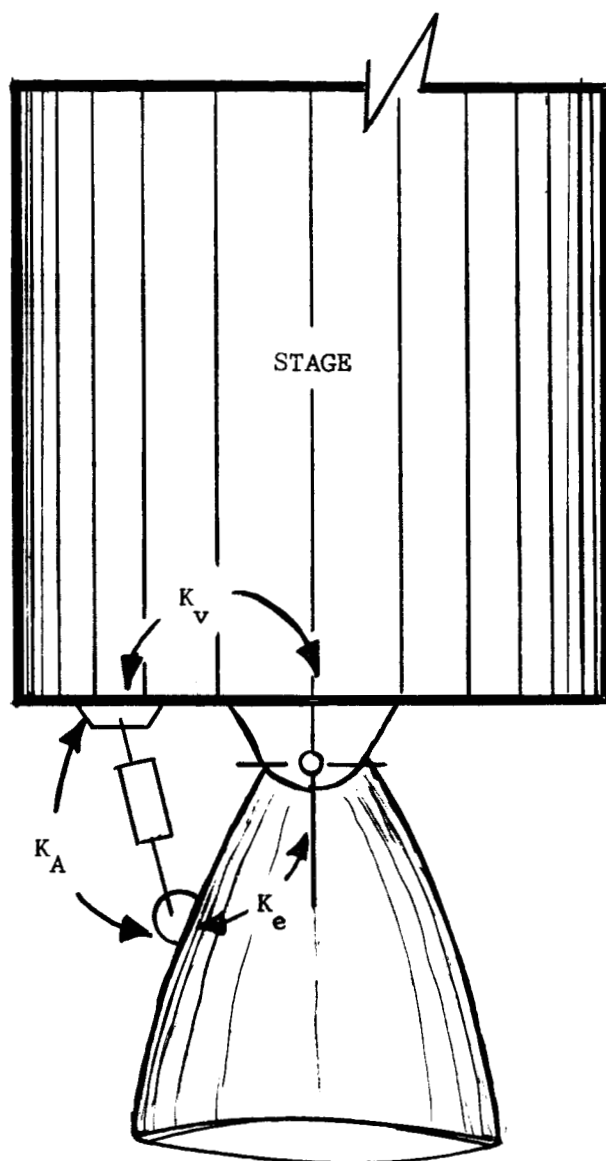


Figure 3. Single engine stage.

afforded him. It is true, however, that the bandwidth of the TVC system is fixed, to a large extent, by the parameters of the stage structure and the engine.

The TVC design engineer will usually be given a performance requirement from the vehicle stage closed loop. The TVC system is expected to contribute only a small part of the vehicle loop phase lag. It is also expected to have a bandwidth that is large with respect to that of the vehicle closed loop. The amplitude ratio of the TVC system is expected to be relatively flat throughout the bandwidth of the vehicle.

The design engineer is faced with many early decisions and must continually monitor the vehicle development changes. He must be in the information loop on all design changes of the engine, the stage structure, and the vehicle mission requirements. Some of the factors that influence the design are listed and discussed below:

A. Static Loads on Actuator

1. Aerodynamic loading on an engine moving into an air stream.
2. Acceleration forces on the engine if the C.G. is not on the geometric center line of the engine.
3. Moments on the engine due to turning rates of the vehicle.
4. Forces due to lateral accelerations of the vehicle.
5. Friction forces on the engine and actuator moving parts.
6. Engine heat shield loads.
7. Engine duct loads.

8. The thrust vector lateral offset from the gimbal center.
9. Loads due to choked air flow between the engines in a multi-engine configuration.

All these factors must be considered in determining the maximum force capability of an actuator. The maximum force is a very important design parameter because it will affect the weight and cost of the unit. The hydraulic pressure must be kept within the state of the art on pumps, accumulators, reservoirs flex hoses, fittings, etc. Once the pressure has been determined, the piston area is also fixed. The maximum force that can be developed is the piston area times the supply pressure.

B. Velocity

When it has been determined how fast the vehicle must be capable of turning for stability reasons, the maximum velocity of the actuator can be evaluated. A duty cycle can be formulated for the worst conditions for a given vehicle flight. This is usually after stage separation for a multi-stage vehicle. A detailed evaluation of worse conditions may be necessary to determine this duty cycle. This will furnish the control engineer enough information to determine the maximum volume of an accumulator, and the rate of the actuator piston. He may want to include safety factors, consistent with good design, in making his final decision on the maximum design velocity of the TVC system.

C. Maximum Actuator Stroke

Once the attach points have been located on the engine and the maximum angular deflection of the engine has been determined one can

size the maximum stroke required for actuators. The maximum stroke and the duty cycle of the actuators enable one to determine the required fluid flow for the system. The fluid supply system can now be designed for the thrust vector control system. The maximum stroke plays a large part in the overall envelope dimension for the actuator. One must make the decisions early in a vehicle development program in order to assure that sufficient space has been allocated for the actuator and related equipment.

The purpose of this research is to develop a mathematical model for a space vehicle thrust vector control system and to demonstrate how it can be used in designing a TVC system.

To facilitate the presentation, a list of symbols is given in the following.

<u>SYMBOL</u>	<u>DEFINITION</u>	<u>UNIT</u>
$K_a G_1$	Amplifier Transfer Function	$\frac{\text{mA}}{\text{deg}}$
$K_v G_2$	Servo Valve Transfer Function	$\frac{\text{in}^3/\text{sec}}{\text{mA}}$
$\frac{HG_3}{A}$	Actuator Transfer Function	$\frac{\text{deg}}{\text{in}^3/\text{sec}}$
G_4	Reflected Load Transfer Function	$\frac{\text{deg}}{\text{deg}}$
G_5	Load Transfer Function	$\frac{\text{deg}}{\text{deg}}$
G_6	Closed Loop Transfer Function of β_p/β_c	$\frac{\text{deg}}{\text{deg}}$
G_7	Transfer Function of β_E/β_c	$\frac{\text{deg}}{\text{deg}}$

F_o	Open Loop Transfer Function	$\frac{\text{deg}}{\text{deg}}$
K_o	Open Loop Gain	$\frac{1}{\text{sec}}$
I	Valve Current	mA
ϵ	Error Signal	deg
Q	Valve Flow Output	$\frac{\text{in}^3}{\text{sec}}$
β_i	Ideal Piston Position-- β Piston Unloaded	deg
β_p	Actual Piston Position; also, Actuator Position Feedback	deg
β_e	Engine Position	deg
β_c	Command Position	deg
s	Laplace Operator	$\frac{1}{\text{sec}}$
H	Conversion Factor	$\frac{\text{deg}}{\text{in}}$
f	Frequency	Hertz
q	Total Flow to Hydraulic Amplifier	$\frac{\text{in}^3}{\text{sec}}$
q_1	Flow to Valve Spool Ends	$\frac{\text{in}^3}{\text{sec}}$
q_2	Flow through Valve Nozzle	$\frac{\text{in}^3}{\text{sec}}$
α	Flapper Angular Position	Deg.
C_1	Conversion Constant	in^2

C_2	Conversion Constant	#/Deg.
P_1	Spool End Pressure	#/in ²
P_2	Spool End Pressure	#/in ²
P_1	Actuator Piston Pressure	#/in ²
P_2	Actuator Piston Pressure	#/in ²
a	Spool End Area	in ²
A'	Actuator Piston Area	in ²
P_s	System Supply Pressure	#/in ²
b	Servo Valve Spool Damping	#/rod/sec
X	Valve Spool Position	in
K_e	Engine Spring Constant	#/in
K_v	Vehicle Spring Constant	#/in
K_A	Actuator Spring Constant	#/in
K_L	Actuator Load Spring Constant	#/in
K_T	Total Spring Constant $\frac{K_L K_o}{K_L + K_o}$	#/in
K_o	Hydraulic Oil Spring Constant	#/in
R	System Low Return Pressure	#/in
C_1 & C_2	Control Ports from Servo Valve	---
Q_1	Shaping Network Flow from C Caused by $P_2 > P_1$	$\frac{\text{in}^3}{\text{sec}}$

Q_1 & Q_2	are equal for the same value of θ	
K	Shaping Network Spring Rate	#/in
θ	Shaping Network Spool Displacement	in.
\emptyset	Shaping Network Spool Displacement	in.
M	Mass of Spool in Shaping Network	slugs
C_o	Shaping Network Orifice Coefficient	$\frac{\text{\#-sec}}{\text{in}^5}$
A	Shaping Network Spool End Area	in^2
B	Shaping Network Damping Coefficient	$\frac{\text{\#-sec}}{\text{rad.}}$
T_E	Torque Caused by Electrical Current	# - in
T_m	Torque Caused by Permanent Magnets	# - in
T_{ft}	Torque Caused by Flexure Tube Spring	# - in
T_n	Torque Caused by Nozzle Pressure	# - in
T_w	Torque Caused by Feedback Wire	# - in
k	Feedback Spring Constant	#/in

CHAPTER II

TORQUE MOTOR

The torque motor is the unit that converts the electric signal to a mechanical signal which in turn produces the hydraulic signal. Because of the interface between the hydraulic system and the electrical control computer, it is a vital link in the thrust vector control system.

There are many arrangements that one may consider for the torque motor. The best may depend on a specific application. The one that will be considered here is shown in Figure 4.

The sides are permanent magnets arranged so that the poles will be located as shown in the Figure 5. The top of the torque motor is soft iron or any material suitable to contain magnetic flux. A side view is shown in Figure 6. The armature of the torque motor is spaced in the center of the air gap as shown and held in place by a flexure tube with a spring rate suitable to maintain a null position at zero electrical current. A small electrical signal in the milliamperage range, applied to the coil of the torque motor, will cause forces in the permanent magnetic field to repel and retract. A resulting angular position will occur that is proportional to the magnitude of the electrical signal.

A flapper with one end setting in between two streams of hydraulic fluid, is connected to the bottom of the armature. The flow from the two ports and the nozzle pressures are affected by the position of the

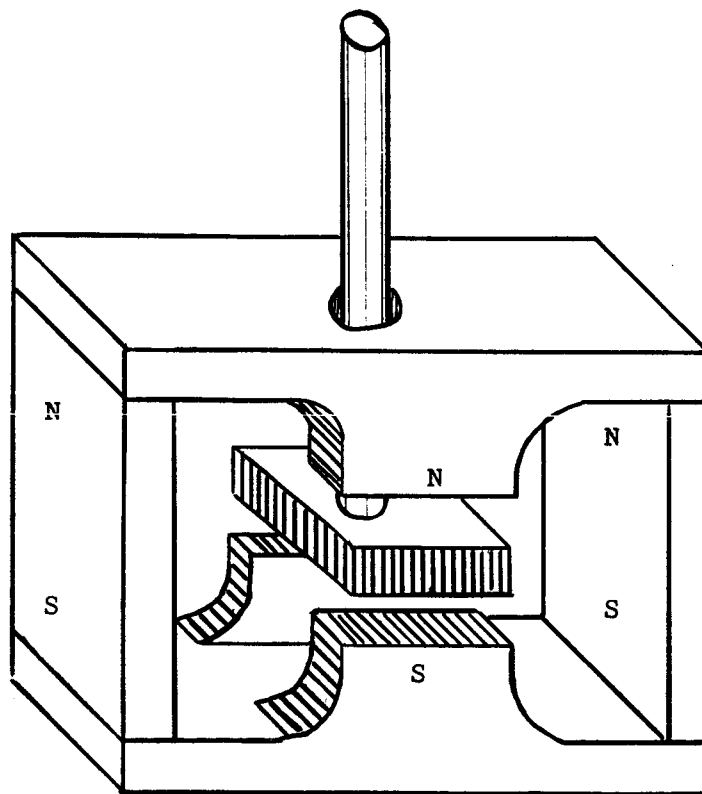


Figure 4. Torque motor armature and magnets.

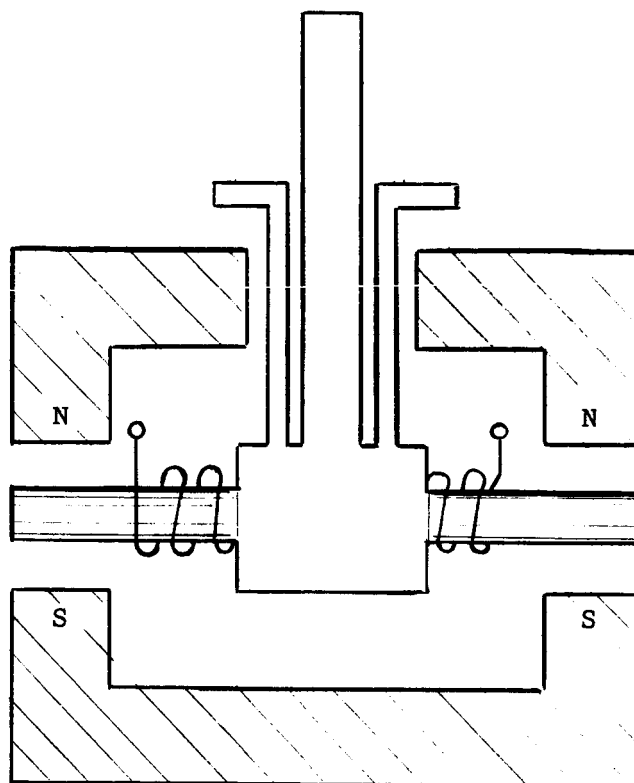


Figure 5. Side view of torque motor.

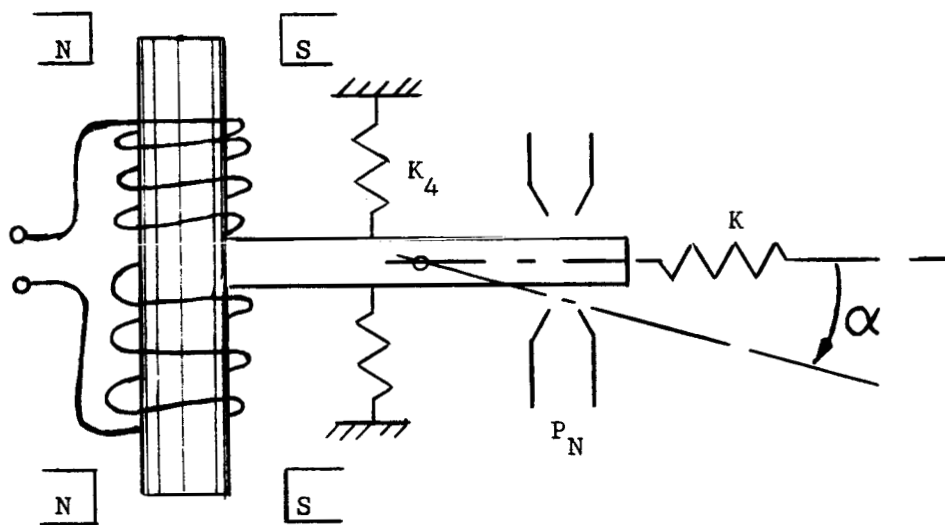


Figure 6. Torque motor schematic.

flapper. As the flapper angle α increases from the null position, the pressure P_n against the flapper increases, thus causing a resisting torque to the electrical current torque. One must be careful not to space the nozzle parameters so that the "flat plate" characteristics (5)* of the flapper tend to pull the flapper toward the nozzle instead of repelling. This characteristic is a positive feedback term. When it occurs, it is destabilizing. The constant of proportionality K_3 between the angular position and the nozzle torque will have a negative sign associated with it.

The flapper and armature arrangement is used as a free body.

Setting the resultant torque to zero, gives

$$T_E + T_m = T_{ft} + T_n + T_w$$

Assuming the proportional relationships

$$T_E = K_1 i$$

$$T_m = K_2 \alpha$$

$$T_n = K_3 \alpha$$

$$T_{ft} = K_4 \alpha$$

and

$$T_w = K_5 \alpha$$

where K_1 , K_2 , K_3 , K_4 and K_5 are real constants, one has

$$K_1 i = (K_4 + K_3 + K_5 - K_2) \alpha$$

* Numbers in parentheses represent similarly numbered entries in the "List of References."

Therefore,

$$\frac{\alpha}{i} = \frac{K_1}{(K_4 + K_3 + K_5 - K_2)} \quad (1)$$

Design feedback wire so that the torque caused by the spring constant K_5 and the angular displacement α is neglectable.

$$\frac{\alpha}{i} = \frac{K_1}{(K_3 + K_4 - K_2)} \quad (2)$$

The desired angular position is shown to be proportional to the value of the electrical current.

If the amplifier is a voltage source then the # block must be evaluated (Figure 7). One will get a back emf generated any time the torque motor armature moves because it is setting in a magnetic field. This can be a source of noise, especially if some of the mechanical resonant frequencies are in the bandpass of the amplifier.

CHAPTER III

SERVO VALVE

The torque motor will produce an angle α proportional to the current through the coil windings. For a given non-zero angle, the flapper will be closer to one nozzle than the other. A continuous flow of hydraulic fluid is moving from the nozzles to the low pressure area surrounding the flapper. The nozzle that is closest to the flapper will have an increase in pressure thereby restricting the fluid flow. The fluid flow q , see Figure 8, will remain constant and is equal to $q_1 + q_2$. Since q_2 has decreased because of the high pressure, caused at the flapper, the value q_1 must increase. Anytime the value of q_1 is greater than zero, the valve spool must move. The spool position X will change to increase the volume to provide space for the flow of q_1 . The spool will continue to move and take with it one end of the feedback spring. As X increases the flapper will be forced away from the nozzle and the pressure will drop causing q_2 to increase. As q_2 increases, q_1 will decrease and when it has dropped to zero, the spool will come to a rest position. Since the electrical torque is still present at the torque motor, it is being nulled out by the torque caused by the spring constant times the displacement X of the spool.

The electrical current may be brought to zero and the electrical torque will be removed. When this happens, the flapper will move to the opposite nozzle and raise the pressure causing q_3 to decrease. As q_3

decreases, the values of q_4 will increase causing the spool to move in the $-X$ direction. As the spool moves, it will reposition the flapper to the null position. The spool will again assume a rest position.

It can be seen, in Figure 8, that for each displacement X the value spool will open a port permitting hydraulic fluid to flow from the high pressure region P_s to one of the control ports C_1 to C_2 . For a positive value of X , fluid will flow to the C_2 port and to the actuator. This is usually a large quantity of flow compared to other flows considered up to now. It has been established that the static value of X is proportional to the valve current. This is a good feature, however, the flow to the actuator is the desired output of the servo valve. The value of fluid flow through an orifice, see Figure 9, is not proportional to displacement only. The flow is a function of the differential pressure across the orifice. The value of the pressure drop is a function of the orifice coefficient - which is a variable in this case - not a constant. Figure 10 shows the relationship between the flow rate Q and the differential pressure ΔP . If one restricts the valve to small values of flow, the relationship is almost a straight line. (See Figure 11.)

The flow to the actuator is also a function of the down stream pressures. The pressure, or differential pressure, across the actuator will determine the amount of fluid flow. This is a result of the fluid compressibility. If the fluid was incompressible, the displacement of the actuator piston would be an exact integral of the flow. A set of curves indicating the flow characteristics of the servo valve may be

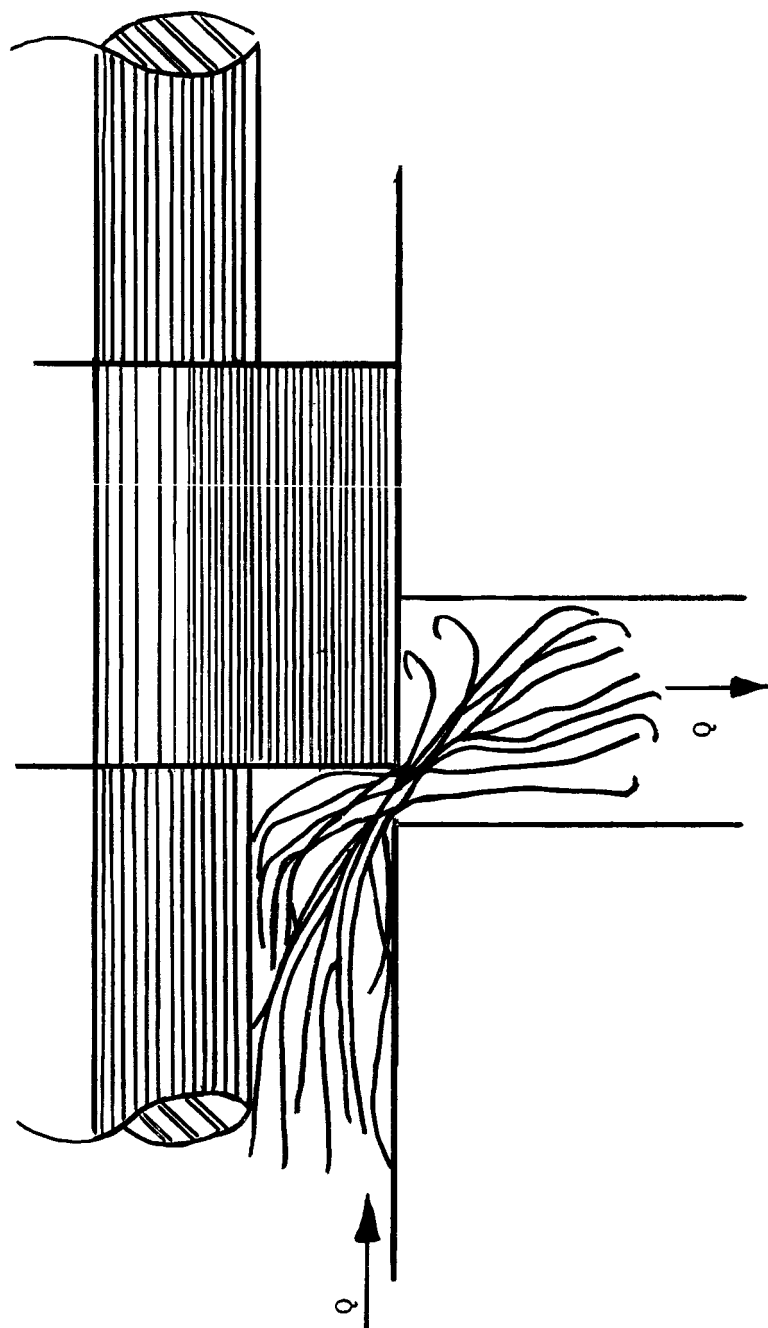


Figure 9. Variable sharp edge orifice.

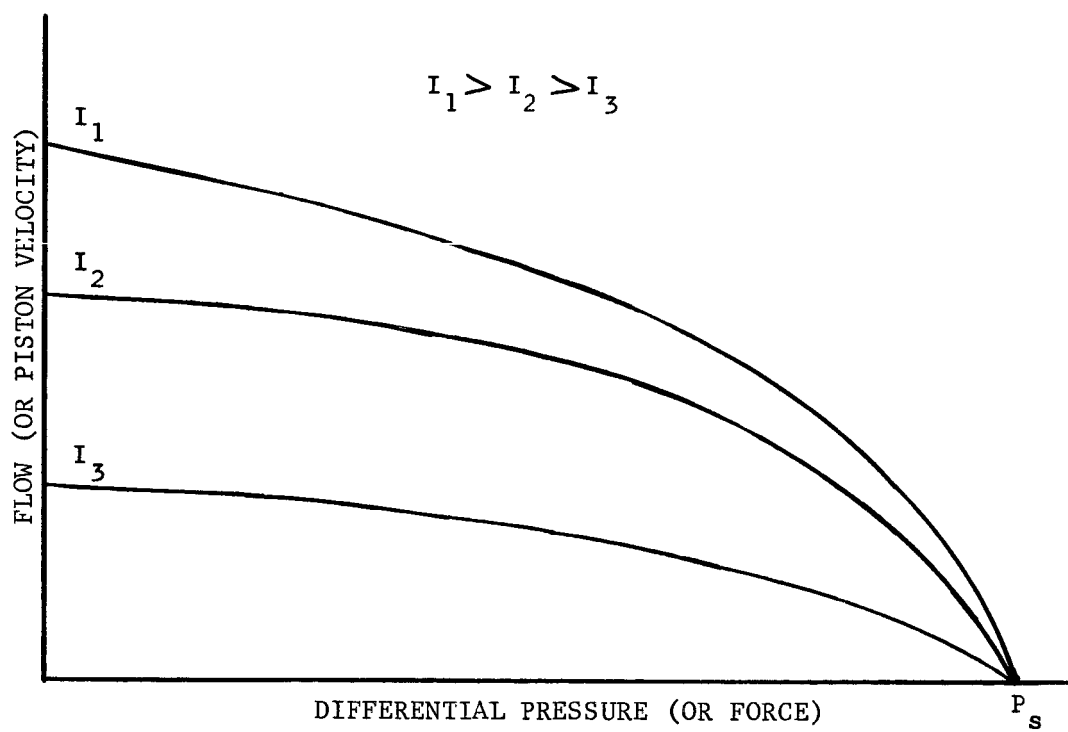


Figure 10. Servo valve flow curves.

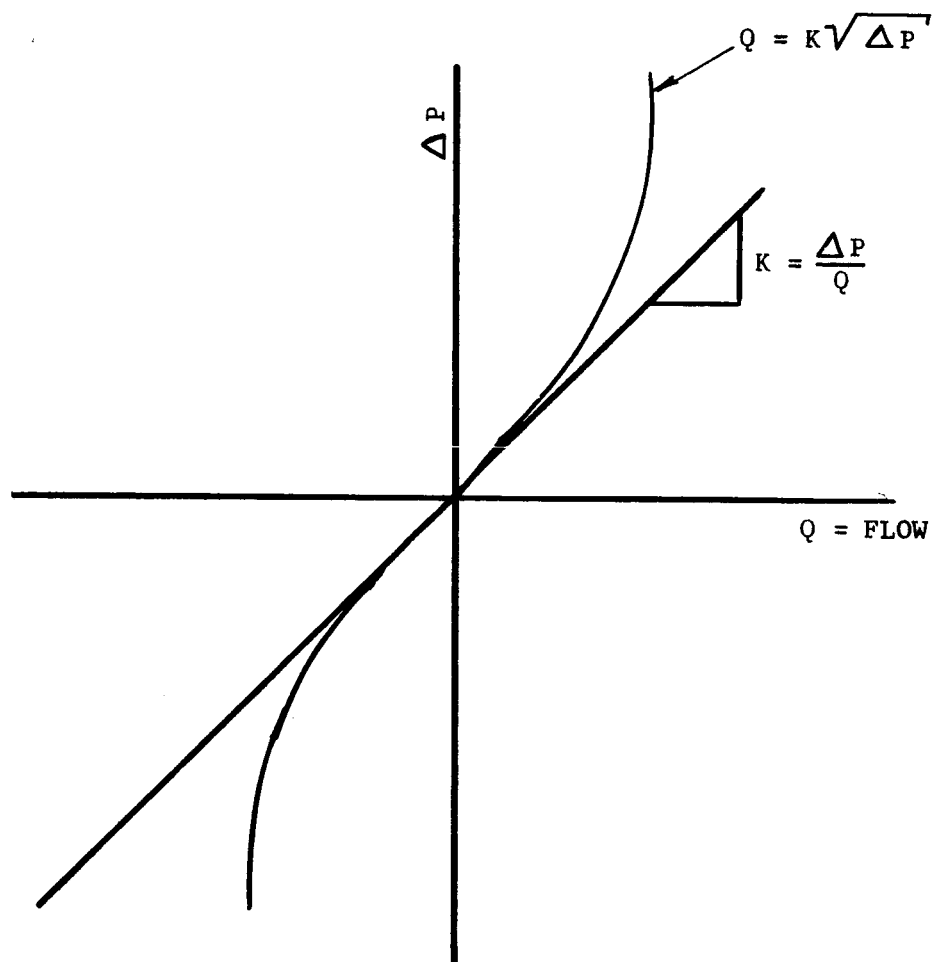


Figure 11. Sharp edge orifice curves.

obtained by observing the three parameters Q , ΔP , and the valve current i . A set of curves is shown in Figure 10.

The piston velocity is obtained by dividing the valve flow by the actuator piston area. The torque, or the available force capability, can also be shown on the same graph. This curve can give the necessary information to design the flow requirements of the valve but is not the full picture of these relationships. A more complete picture is shown in Figure 12, a four quadrant picture of these characteristics. The negative flow of the valve takes into account the direction of flow through the C_1 and C_2 ports to the actuator. This figure also indicates the flow relationship if the load causes a pressure that is out of phase with the valve signal. This can cause the differential pressure of the actuator to be larger than that of the system supply. This should not happen in practice, however, the curves can be produced by operating the hardware in the laboratory.

The relationship of fluid flow to valve current and the differential pressure is a nonlinear relationship. However, if one holds the differential pressure constant and plots a curve of the flow vs current from the curves of Figure 10, one obtains a family of curves as those in Figure 13. This is the most useful set of curves since the slope of the straight line is the flow gain of the valve and is a large part of the open loop gain. One must choose the largest slope in determining the open loop gain for sizing the thrust vector control system. This will also be the correct value for small signal operation.

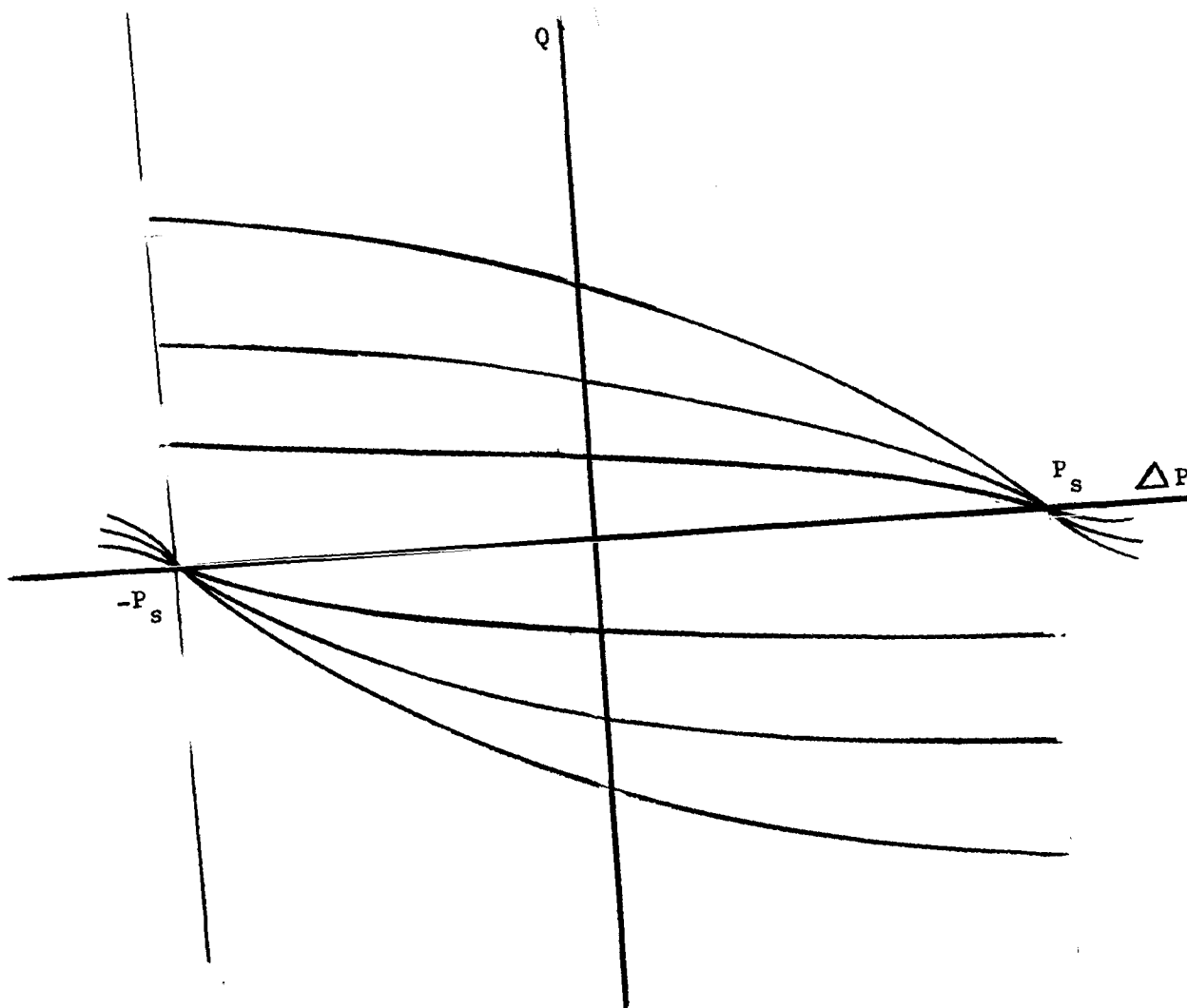


Figure 12. Four quadrant flow curves.

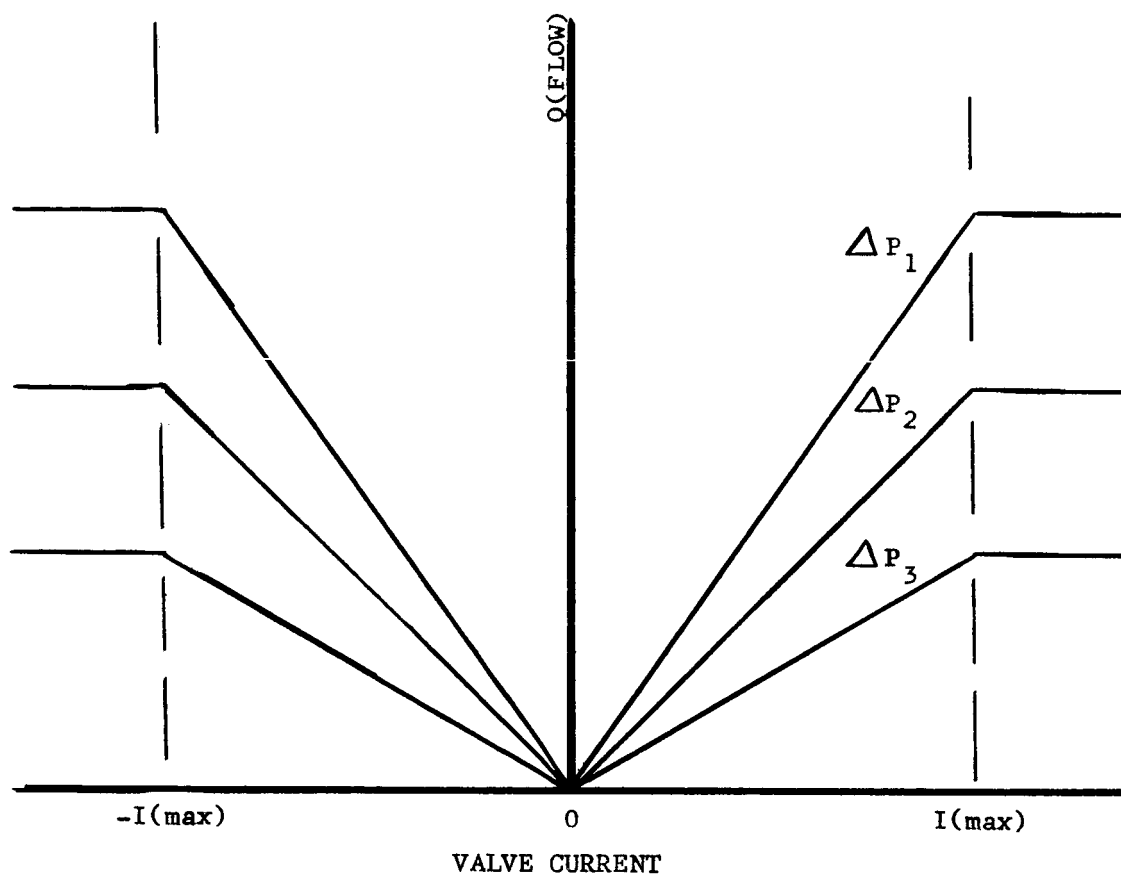


Figure 13. Linear flow curves.

In developing the mathematical relationships of the valve, one needs to simplify the block diagram of Figure 7, page 18. A more useful block diagram would be to start with that of Figure 14. This figure gives a picture of the signal flow paths and the parts of the system that operate on the signals. It is difficult to see the parameter relationship of the valve from this figure. One can start with Figure 8, page 20, and develop force and flow equations.

Considering the schematic in Figure 8 and assuming flow continuity, it can be stated that $q = q_1 + q_2$. Since a pipe or an orifice has some resistance to fluid flow, there will be a pressure drop along the tube. This can be expressed as

$$c_1(p_s - p_1) = q_2 \quad . \quad (3)$$

For small changes in fluid flow c_1 is approximately a constant. This is a valid assumption since q is small and q_2 is never zero and has as its maximum value q . Also, q_2 is a function of the orifice caused by the nozzle and the flapper. The flapper position α causes a restriction to flow and is expressed

$$q_2 = c_2 \alpha \quad . \quad (4)$$

Setting the two equations equal

$$c_1(p_s - p_1) = c_2 \alpha$$

and

$$p_1 = p_s - \alpha \frac{c_2}{c_1} \quad . \quad (5)$$

The relationship of flow to the flapper angle $-\alpha$ is similarly derived

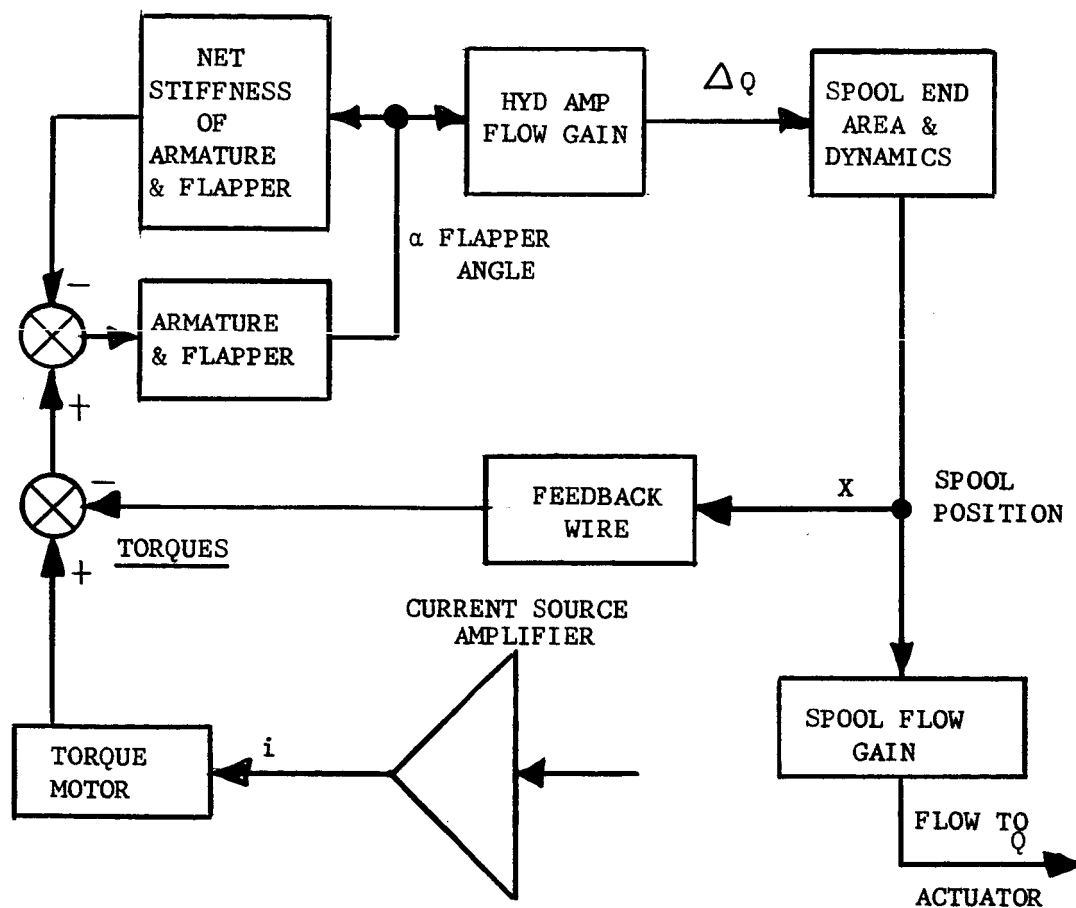


Figure 14. Simplified block diagram.

$$p_2 = p_s + a \frac{c_2}{c_1} \quad (6)$$

By taking the difference of Equations (5) and (6), one can eliminate p_s

$$p_1 - p_2 = -2a \left(\frac{c_2}{c_1} \right) \quad (7)$$

Now it is more convenient to treat the spool as a free body and sum all the essential forces acting on this body, see Figure 15. One can neglect the value of the force caused by the feedback spring kx . This spring is not used to null the valve spool however, it is used to reposition the flapper which changes the flow which does null the spool. The essential forces on the free body diagram are as follows:

$$ap_1 = m\ddot{x} + ap_2 + b\dot{x} \quad .$$

Taking Laplace transform with zero initial condition and transposing one term,

$$\frac{X}{(P_1 - P_2)} = \frac{a}{s(ms + b)} \quad (8)$$

The transfer function between the valve spool position X and the torque motor flapper position a is obtained by substituting Equation (7) into Equation (8) and rearranging the expression.

$$\frac{X}{a} = \frac{-2 \frac{c_2}{c_1} a}{s(ms + b)} \quad (9)$$

The servo-valve can now be represented by the block diagram shown in Figure 16. The flow from the valve is proportional to the valve spool position.

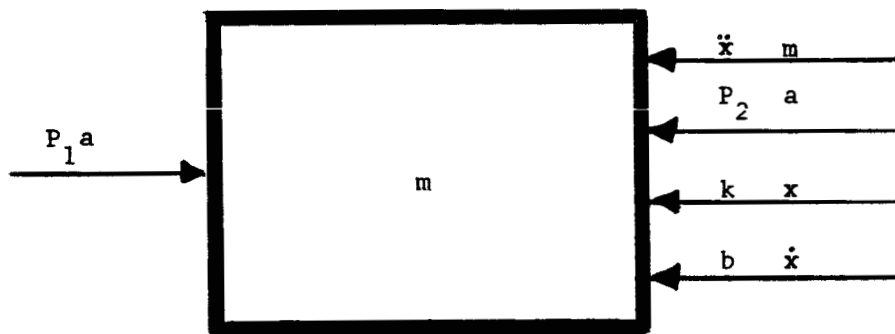


Figure 15. Free body diagram of servo valve spool.

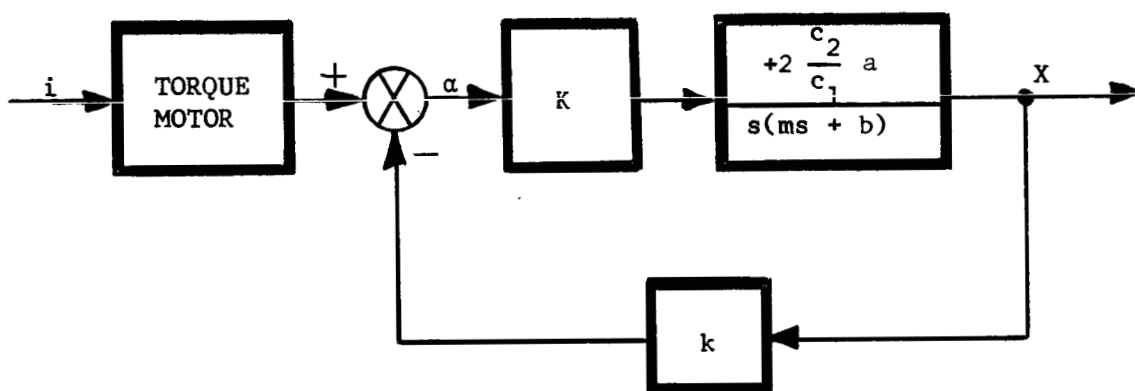


Figure 16. Servo valve block diagram.

CHAPTER IV

LOAD AND REFLECTED LOAD DYNAMICS

The most difficult part of the TVC design problem is the fact that a large spring mass load is outside of the closed loop system. When not controlled by an actuation system, this lightly damped, resonant, second order system, if excited, rings at its natural frequency.

The engine gimbal system is more conveniently dealt with if the system is converted to an equivalent one shown in Figure 17. The mass in this figure is the equivalent mass of the engine converted to linear motion. If the hydraulic fluid was not compressible, the actuator piston position would be β_i . However, the hydraulic fluid is compressible and the true piston position β_p is different from β_i . A feedback potentiometer is located in a favorable position to measure β_p and close the loop around the actuator, servo-valve, and torque motor. The value of K_L is a combination of the compliances of the engine, the vehicle stage structure, and those mechanical parts of the actuator not absorbed into K_O . The springs are not linear but can be approximated as such for small signals.

Since the load is outside the closed loop, one can see that it would be desirable to drive it with a system that has a notch filter located at the natural frequency of the load. This is what is expected of the controls engineer. It turns out that the system has a natural built-in notch if one chooses a hydraulic system. This will be clear in derivation of the system equations.

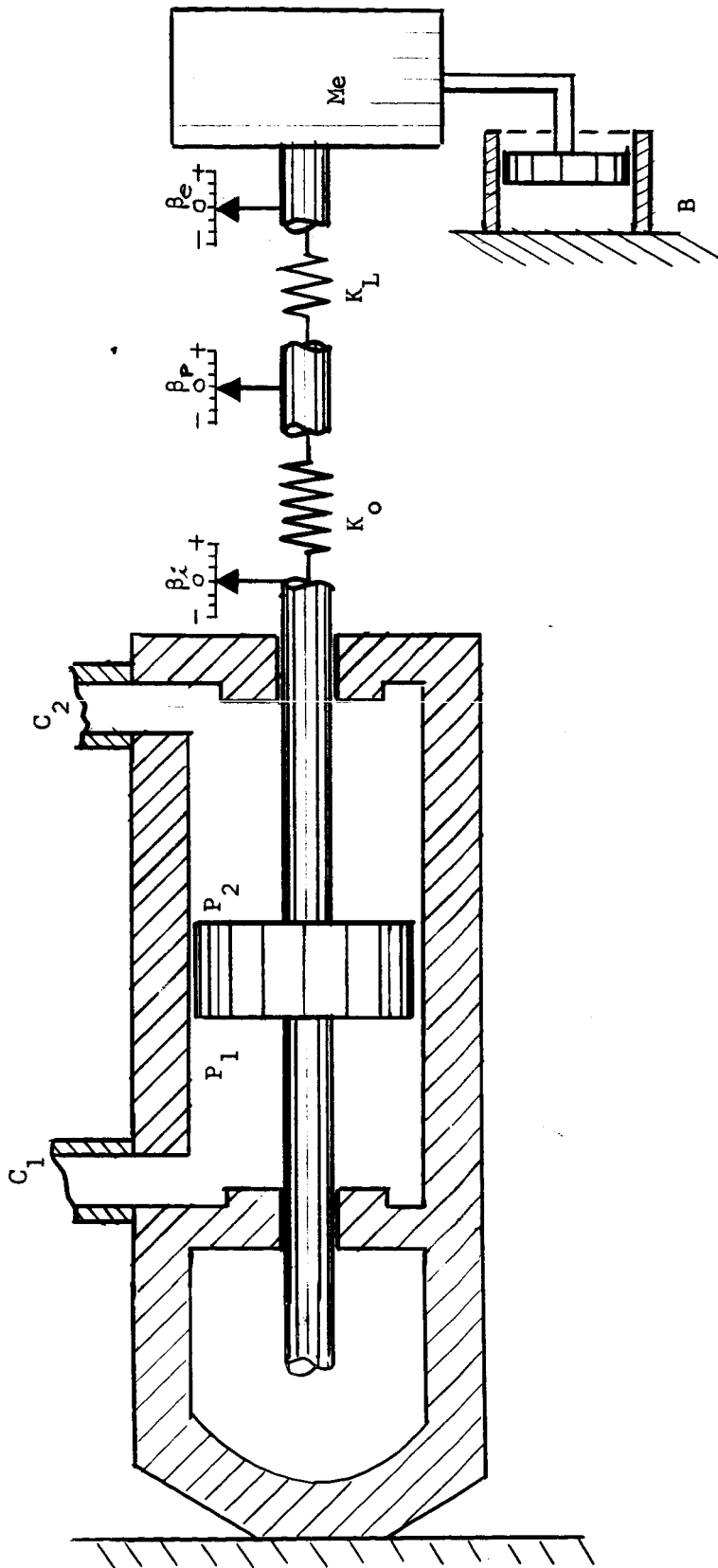


Figure 17. Actuator and load.

One can get a picture of the problem if the spring rate of the oil K_o is assumed to be infinitely stiff. If the servo-valve has ports C_1 and C_2 closed off (see Figure 17), and a disturbance is caused at the load, there will be a displacement at β_e . However, β_i and β_p will not move so there will be no feedback signal. The spring mass system will continue to ring at its natural frequency until the dashpot "B" has dissipated the exertation energy. Since the actual thrust vector is positioned by the geometry of the engine, it is apparent that it will also ring at the natural frequency of the load.

Now if one permits the value of K_o to be a finite value, then for a given force, applied to the engine, the spring will be compressed and cause a β_p displacement. This will cause a feedback signal to be generated and open the servo-valve. The valve will permit flow to reduce the displacement. One can not obtain enough damping as a result of this operation, however, it does cause a notch filter to appear in the equations. The necessary damping or attenuation of the notch filter is obtained by the Dynamic Shaping Network.

In order to derive the equations of motion and obtain workable transfer functions, consider the sketch in Figure 17. If one divides this figure into three free body diagrams and sum all the essential forces, three transfer functions are obtained for the load β_e/β_p , the reflected load dynamics β_p/β_i and β_p/Q . One can observe that the numerator term of β_p/β_i is exactly equal to the denominator term of β_e/β_p . Since β_e/β_p has about 20 db of gain at the resonant frequency,

one would expect β_p/β_i to contribute about the same amount of attenuation at the same frequency. This is exactly what will happen if one can separate the natural frequency of the denominator from that of the numerator terms of β_p/β_i . The frequency response relationship of this transfer function is shown in Figure 18.

From the free body diagrams shown in Figures 19, 20 and 21, the following three equations can be obtained, respectively.

$$(\Delta p)A' = K_o(\beta_i - \beta_p) \quad , \quad (10)$$

$$(\beta_i - \beta_p)K_o = (\beta_p - \beta_e)K_L \quad , \quad (11)$$

and

$$(\beta_p - \beta_e)K_L = m_e s^2 \beta_e + Bs\beta_e \quad . \quad (12)$$

In matrix notation,

$$\begin{bmatrix} (\Delta p)A' \\ 0 \\ 0 \end{bmatrix} = \begin{bmatrix} K_o & -K_o & 0 \\ -K_o & K_o + K_L & -K_L \\ 0 & -K_L & m_e s^2 + Bs + K_L \end{bmatrix} \begin{bmatrix} \beta_i \\ \beta_p \\ \beta_e \end{bmatrix} \quad . \quad (13)$$

The determinant of the system matrix is

$$\Delta = \begin{bmatrix} K_o & -K_o & 0 \\ -K_o & K_o + K_L & -K_L \\ 0 & -K_L & m_e s^2 + Bs + K_L \end{bmatrix} \quad . \quad (14)$$

Solving Equation (13) for β_i , β_p and β_e , yields

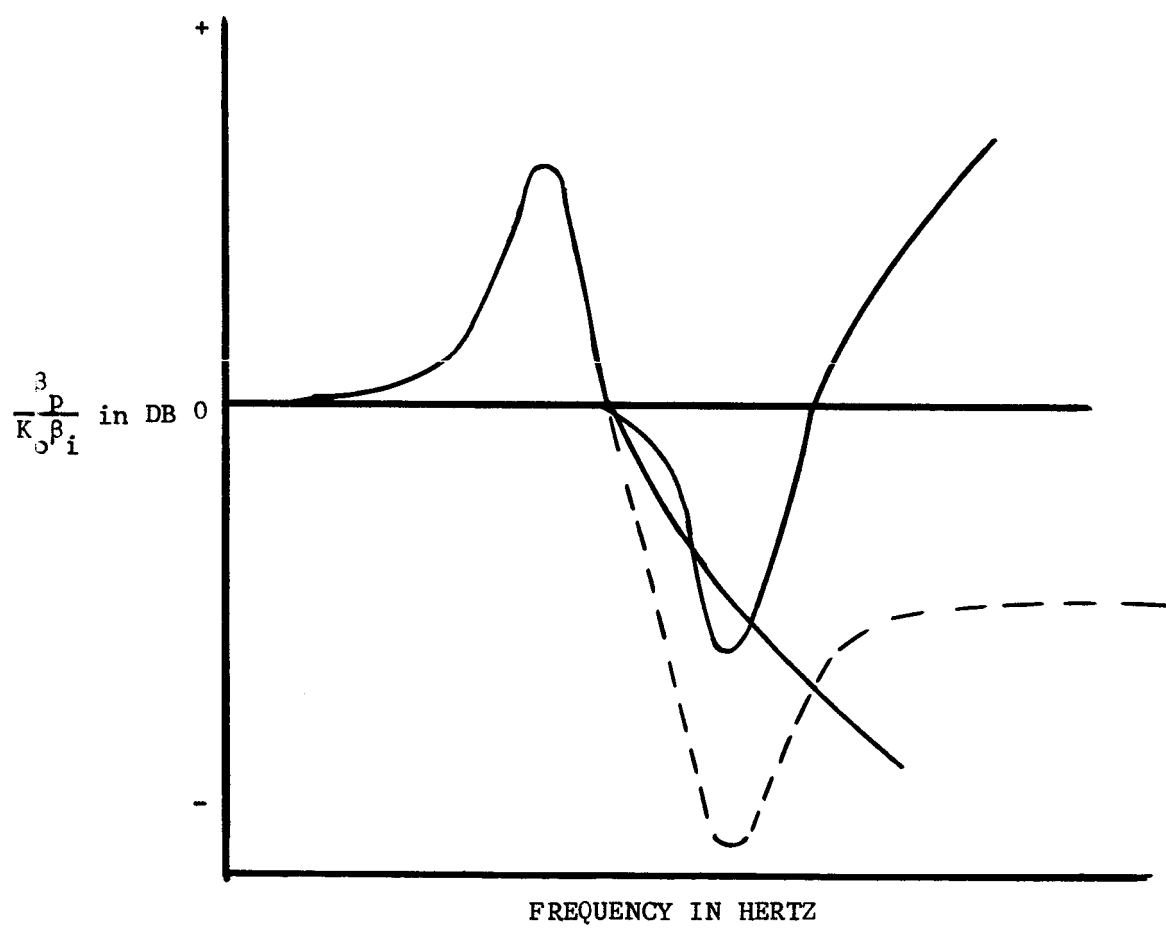


Figure 18. Amplitude response of reflected load.

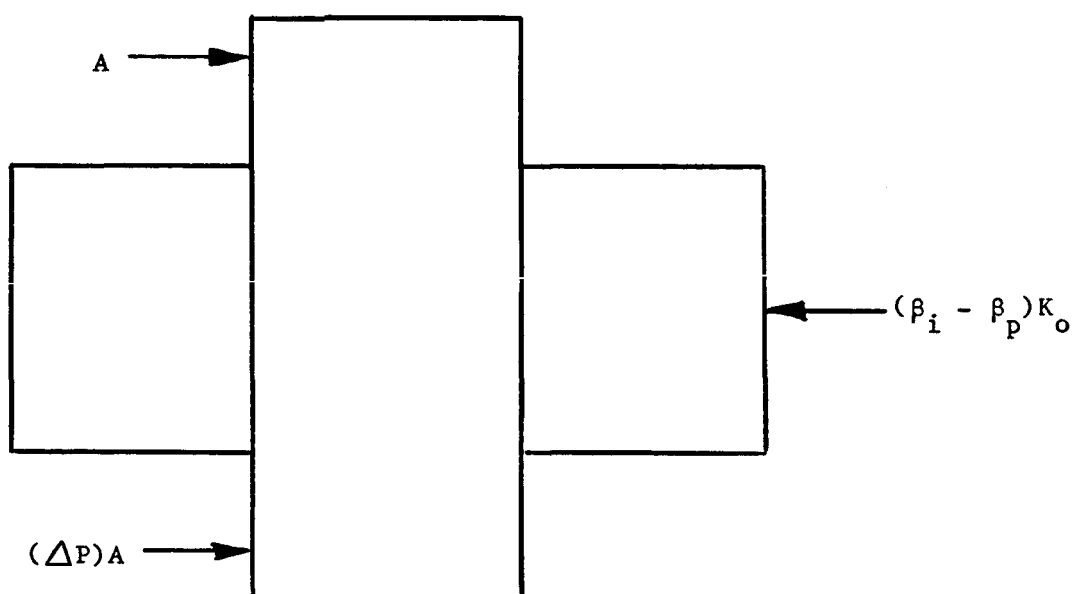


Figure 19. Actuator piston free body diagram.

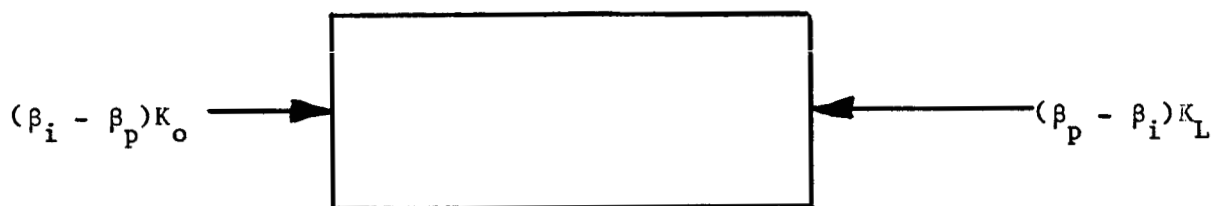


Figure 20. Actuator piston rod free body diagram.

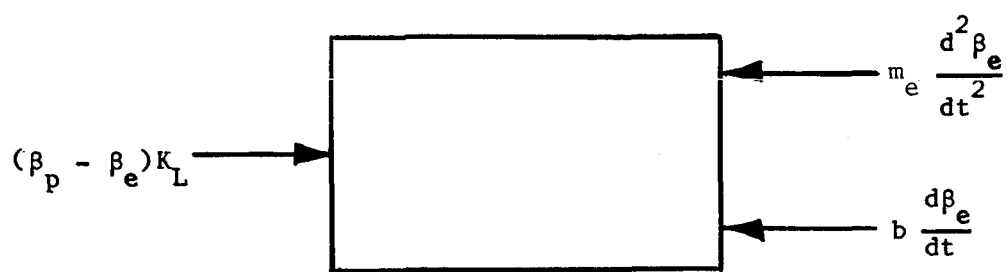


Figure 21. Engine free body diagram.

$$\beta_i = \frac{(K_o + K_L)}{\Delta} \left(m_e s^2 + Bs + \frac{K_o K_L}{K_o + K_L} \right) (\Delta p) A' , \quad (15)$$

$$\beta_p = \frac{K_o}{\Delta} (m_e s^2 + Bs + K_L) (\Delta p) A' , \quad (16)$$

and

$$\beta_e = \frac{K_o K_L}{\Delta} (\Delta p) A' . \quad (17)$$

Thus

$$\frac{\beta_p}{\beta_i} = \frac{K_o}{K_o + K_L} \left(\frac{m_e s^2 + Bs + K_L}{m_e s^2 + Bs + K_T} \right) \quad (18)$$

where

$$K_T = \frac{K_o K_L}{K_o + K_L} < K_L$$

and

$$\frac{\beta_e}{\beta_p} = \frac{K_L}{m_e s^2 + Bs + K_L} . \quad (19)$$

Noting that

$$\beta_i = \frac{1}{A} \frac{Q}{s} ,$$

the relation between the piston and the flow rate is

$$\frac{\beta_p}{Q} = \frac{K_o}{A (K_o + K_L)} \left(\frac{K_L + Bs + m_e s^2}{s (K_T + Bs + m_e s^2)} \right) . \quad (20)$$

Examining Equations (18) and (19), reveals that β_p/β_i always posses a numerator identical to the denominator of β_e/β_p . Thus β_e/β_i

has a natural built-in notch as claimed at the beginning of this Chapter. The hydraulic actuator has the effect of replacing a pair of highly resonant poles of the load by a pair of highly damped poles of the overall system.

CHAPTER V

DYNAMIC SHAPING NETWORK

The dynamic shaping network for the actuation system is made entirely of mechanical components. A schematic of the network is shown in Figure 22. This network is placed between a conventional flow control servo valve and the hydraulic actuator; and, C_1 and C_2 are the connecting parts of the servo valve and actuator. The pressure developed at the faces of the actuator piston is designated P_1 and P_2 . It is assumed to be uniform across the piston face and of the same values at C_1 and C_2 . The differential pressure developed by the actuator is $(P_1 - P_2)$. The sign gives an indication of the direction of the highest pressure.

The equations are developed by summing all the forces acting on a "free body" diagram and setting them equal to zero. A free body of the elements is shown in Figure 23.

If the mechanical components of the shaping network are arranged in the same manner as those shown schematically in Figure 22, one can obtain a derivative of the differential pressure $(P_2 - P_1)$. If the system is in a state of equilibrium and the pressure P_2 is caused to increase, it will cause a displacement ϕ which is equal to $(P_2 - P_3)A/K$. During the time that ϕ is changing, there will be an oil flow rate Q_4 . If this rate is large enough, it will cause the orifice C_0 to look as though it is blocked, and Q_3 will be essentially 0. Therefore, Q_5 will

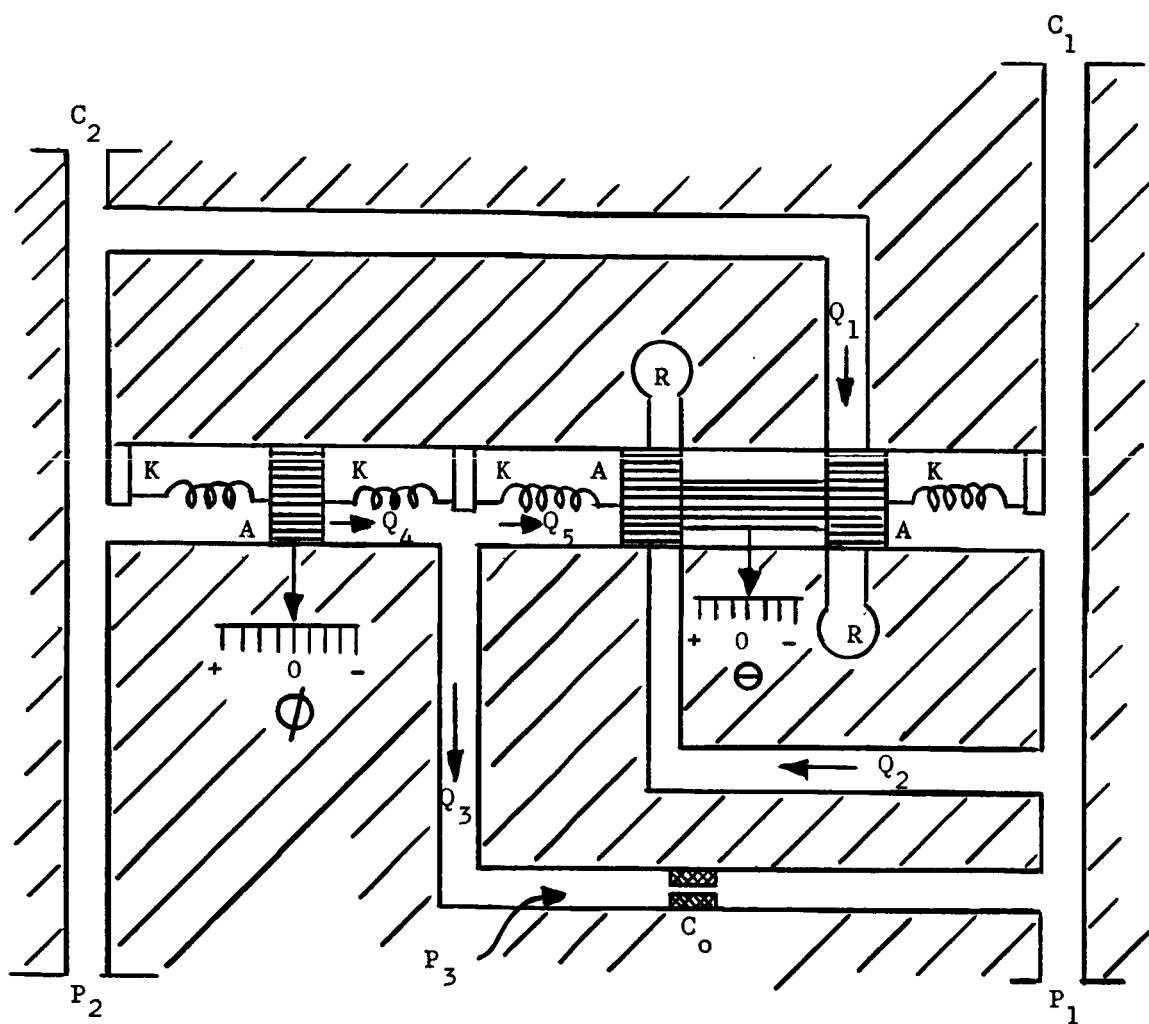


Figure 22. Shaping network schematic.

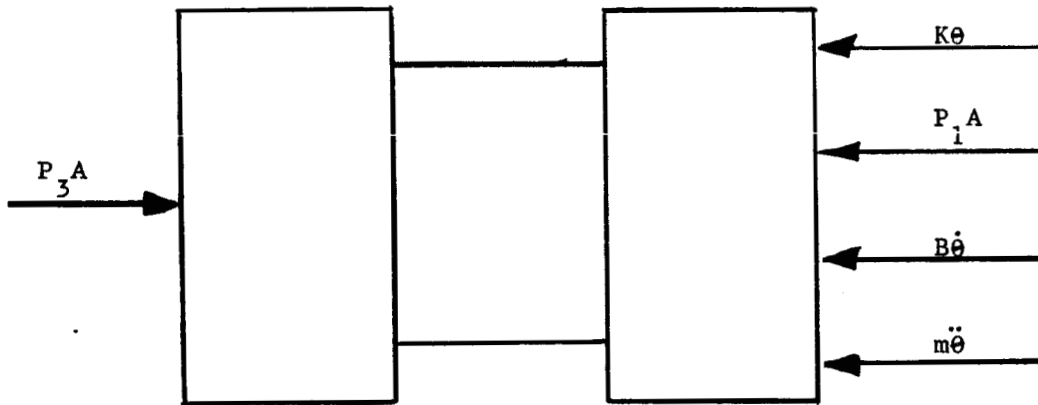


Figure 23. Shaping network free body diagram.

approximately equal to Q_4 . This will cause a displacement θ which is equal to $A(P_3 - P_1)/K$. When θ is in the minus direction, the spool will open a port which permits Q_1 to flow to the low pressure return port R. When this happens, the pressure P_2 will drop. This causes the pressure to have a rate of change that is opposite in polarity to that when it was increasing and thereby closing the port caused by the spool.

If P_1 is increased above that of P_2 , the same operation occurs, but in the reverse direction.

It can be seen that regardless of the level of P_1 and P_2 the spool displacement θ will remain in the neutral position. For a static condition θ may be displaced, however, P_3 will equal P_1 and the forces acting on the spool for θ , will be balanced and fluid flow is possible.

The force Equation for the left spool is

$$(P_2 - P_3)A = (K + Bs + M_1 s^2)\theta$$

For sufficiently small M_1 , a good approximation is

$$\frac{\theta}{P_2 - P_3} = \frac{A}{K + Bs} \quad (21)$$

Similarly, for the right spool, one has

$$(P_3 - P_1)A = (K + Bs + M_2 s^2)\theta$$

For small M_2 , it becomes

$$\frac{\theta}{P_3 - P_1} = \frac{A}{K + Bs} \quad (22)$$

The linearized force equation for the built-in orifice is

$$P_3 - P_1 = C_o Q$$

Using the continuity Equation

$$Q_4 = Q_5 + Q_3$$

and the relationship

$$Q_4 = As\theta$$

and

$$Q_5 = As\theta$$

gives

$$As\theta = As\theta + (P_3 - P_1) \frac{1}{C_o} \quad . \quad (23)$$

Eliminating $(P_3 - P_1)$ from Equations (22) and (23),

$$C_o As\theta - \left[C_o As + \frac{K + Bs}{A} \right] \theta = 0 \quad . \quad (24)$$

Eliminating P_3 from Equations (21) and (22),

$$\frac{K + Bs}{A} \theta + \frac{K + Bs}{A} \theta = P_2 - P_1 \quad . \quad (25)$$

In matrix form,

$$\begin{bmatrix} \frac{K + Bs}{A} & \frac{K + Bs}{A} \\ C_o As & C_o As + \frac{K + Bs}{A} \end{bmatrix} \begin{bmatrix} \theta \\ \theta \end{bmatrix} = \begin{bmatrix} P_2 - P_1 \\ 0 \end{bmatrix} \quad . \quad (26)$$

Solving Equation (26) for θ , gives

$$\frac{\theta}{P_2 - P_1} = \frac{-AC_o}{2BC_o + \frac{B^2}{A^2}} \left[\frac{s}{s^2 + \frac{2 \left(C_o K + \frac{BK}{A^2} \right)}{\left(2C_o B + \frac{B^2}{A^2} \right)} s + \frac{K^2}{A^2 \left(2C_o B + \frac{B^2}{A^2} \right)}} \right] \quad . \quad (27)$$

It is desirable to approximate Equation (27) in a form having one s factor in the numerator and only one time constant in the denominator. This can satisfactorily be done if Equation (27) has two real poles, one at least ten times larger than the other.

Letting

$$\alpha = C_o B + \frac{B^2}{A^2} \quad ,$$

the characteristic Equation of Equation (27) becomes

$$s^2 + \left(\frac{2 \frac{K}{B} \alpha}{C_o B + \alpha} \right) s + \frac{K^2/A^2}{C_o B + \alpha} = 0 \quad .$$

The roots of this Equation is

$$s = \frac{K\alpha}{B(C_o B + \alpha)} \left(-1 \pm \frac{1}{\alpha} \sqrt{\alpha^2 - \frac{B^2}{A^2} (C_o B + \alpha)} \right) \quad .$$

After simplification, one arrives at the following two roots

$$\begin{aligned} s_1 &= -\frac{K}{B} \\ s_2 &= -\frac{K}{B} \gamma \end{aligned} \quad , \quad (28)$$

where the factor γ is given by

$$\gamma = \frac{B}{B + 2C_o A^2} \quad . \quad (29)$$

Thus Equation (27) may be written as

$$\frac{\theta}{P_2 - P_1} = \frac{-C_o A}{2C_o B + \frac{B^2}{A^2}} \left(\frac{s}{(s + \frac{K}{B})(s + \frac{K}{B} \gamma)} \right) \quad . \quad (30)$$

To separate the two roots the desired amount, γ can be adjusted. Notice that $\gamma < 1$, since B , C_o and A are all positive. Also, $\frac{K}{B}$ is set so that it will be large compared to the system band width.

In order to adjust γ one can change the value of C_o which is an orifice in the hydraulic circuit. The spool area may be set due to other constraints. The contaminant small particle size may play a large part in determining the size of the piston area. Also, the larger the value of K the more force will be required to obtain a reasonable amount of θ ; therefore, this will also help to determine the size of the area.

A frequency response of a satisfactory network is shown in Figure 24.

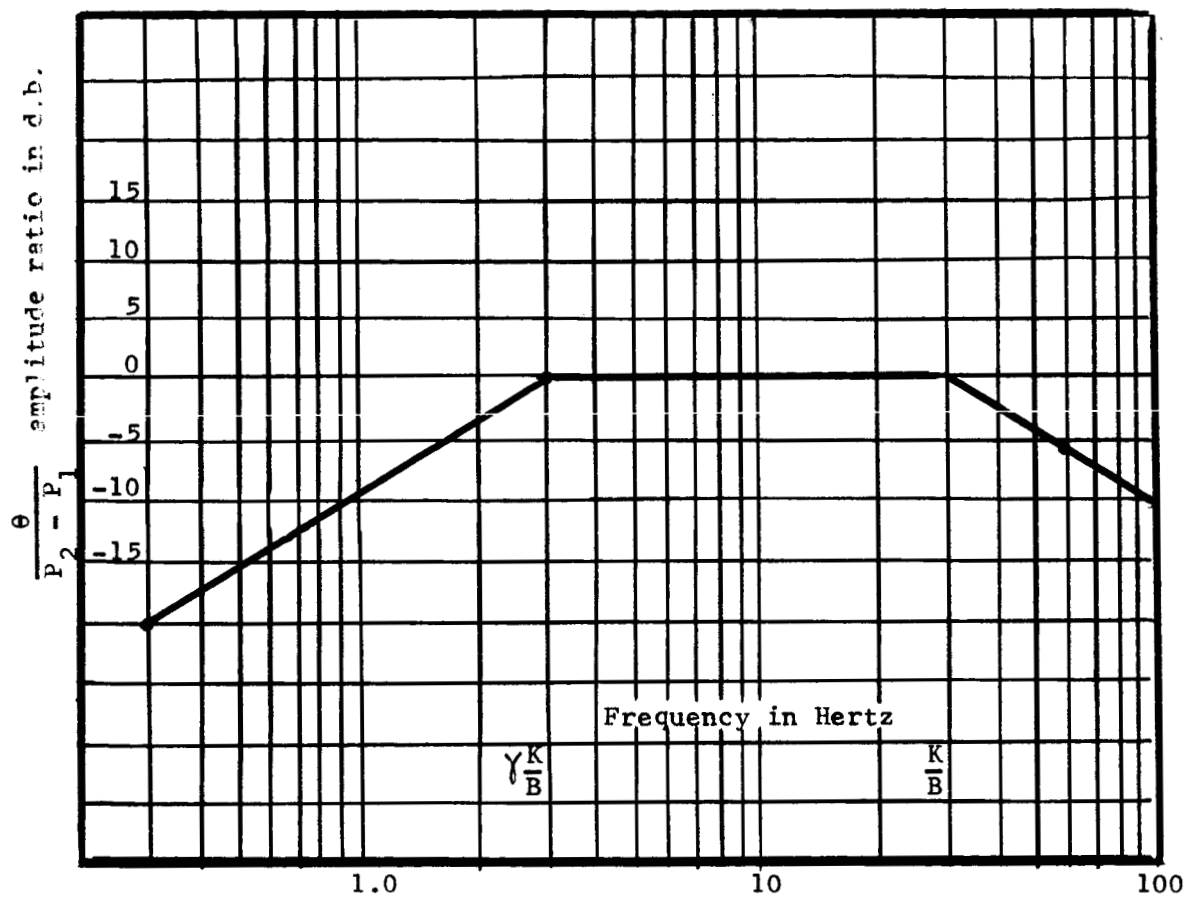


Figure 24. Frequency response of network.

CHAPTER VI

SUMMARY

The equations of motion for the various components of the thrust vector control system have been developed in the preceding chapters. The schematic of Figure 25 shows how these various subsystems combine to form a TVC system. This particular shaping network enables one to design a system by the use of conventional flow valves and actuators. When it is possible to use hydraulic fluid, as the working medium, one is afforded many advantages that are not available by other actuation systems. The dynamic load shown by β_e/β_p in Figure 26 has approximately 20 db of gain at the resonant frequency. The closed loop hydraulic system is shown to be β_p/β_c and gives a considerable amount of attenuation at the load resonant frequency. The desired response of the combined curves is shown as β_e/β_c . One can see that this has the response of a well controlled stable system.

For multiple engine control, hydraulic system is the most versatile. In a multiengine control system, it is desirable from a hardware viewpoint, to design one TVC system that can be interchangeable from engine to engine. Because of the tolerance used in manufacturing the stage structure, the engine, torque motor, servo-valve, and the actuators, it is difficult to predict exactly what the resonant frequency of the load will be. A hydraulic fluid system will alleviate this problem to a large extent. The natural frequency of the system used in Figure 26 was changed

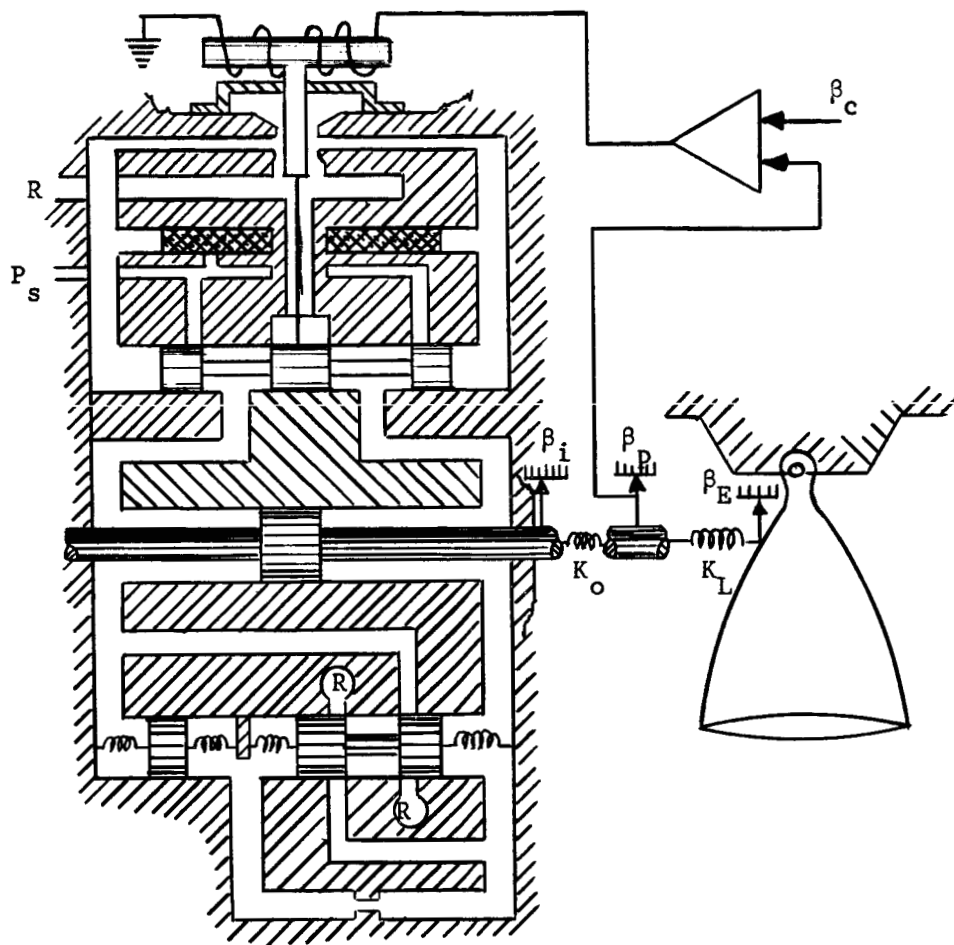


Figure 25. Schematic of complete T.V.C..

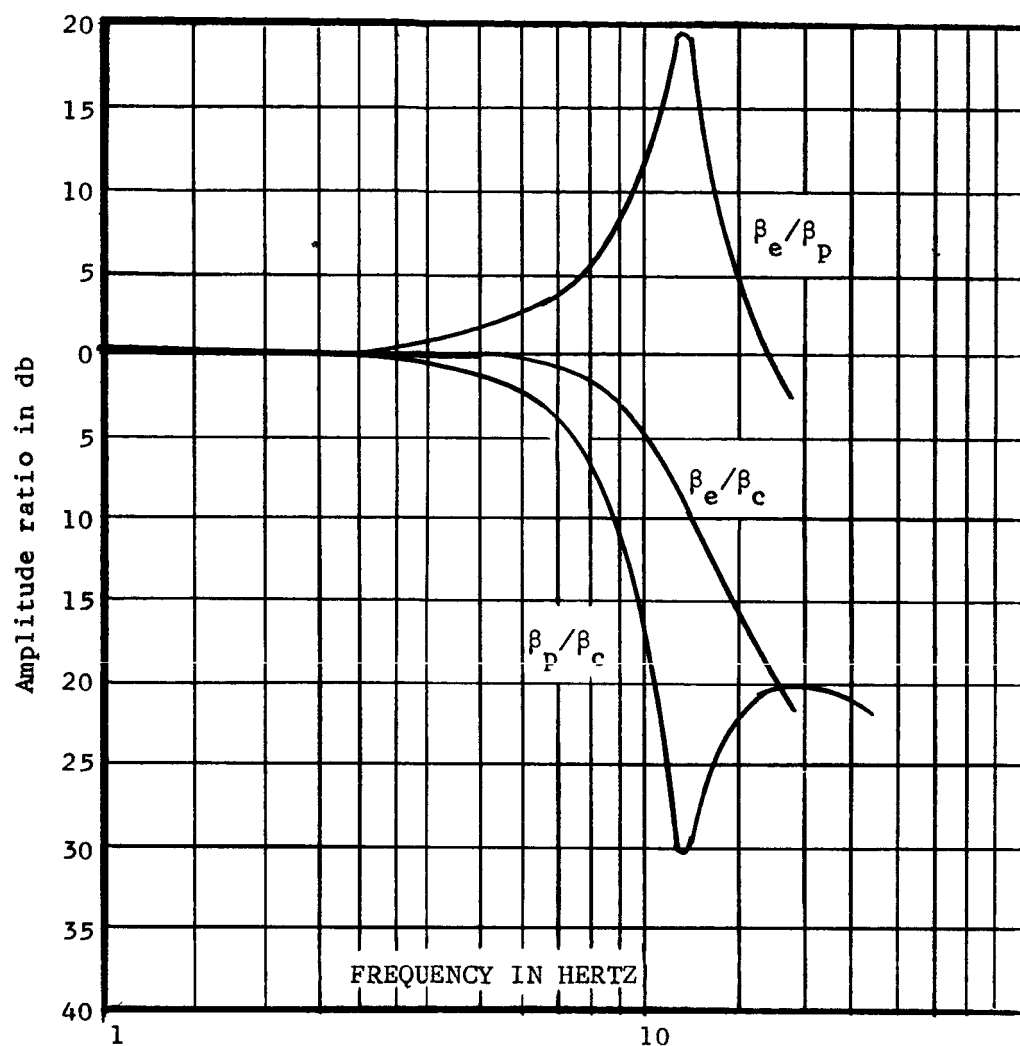


Figure 26. System frequency response.

to new values and the curves of Figure 27 and Figure 28 were obtained. When the load response changed, the TVC system notch changed to the new value dictated by the load. Although the attenuation of the closed loop system was not as much, the notch frequency was automatically the desired one. This is caused by the fact that the numerator term of the reflected load has coefficients that are exactly the same as those of the load. One can see by Figure 28 that the response β_e/β_c changed only slightly although the load response changed by several Hertz. This is the response that one is primarily interested in since it is that of the actual thrust vector.

The mathematical models developed may be arranged into a block diagram such as that shown in Figure 29. This is the most convenient form to set up on an analog computer for the ease of parameter adjustments.

If one is to meet the closed loop phase requirement of the TVC system, the open loop again will make the largest change in the phase curve at low frequencies. However, when the phase requirement is met the amplitude ratio may not be what one desires.

The set of curves in Figure 30 show some degree of adjustment available by adjusting the parameters in the shaping network. One can move the saddle, formed by the set of curves, up or down by adjusting the break frequency ($\gamma \frac{K}{B}$). One can move from one curve to the other by adjusting the gain of the pressure feedback loop. The higher frequency phase lag will change but will remain relatively constant at low frequencies. The data in Figure 31 was taken from analog runs.

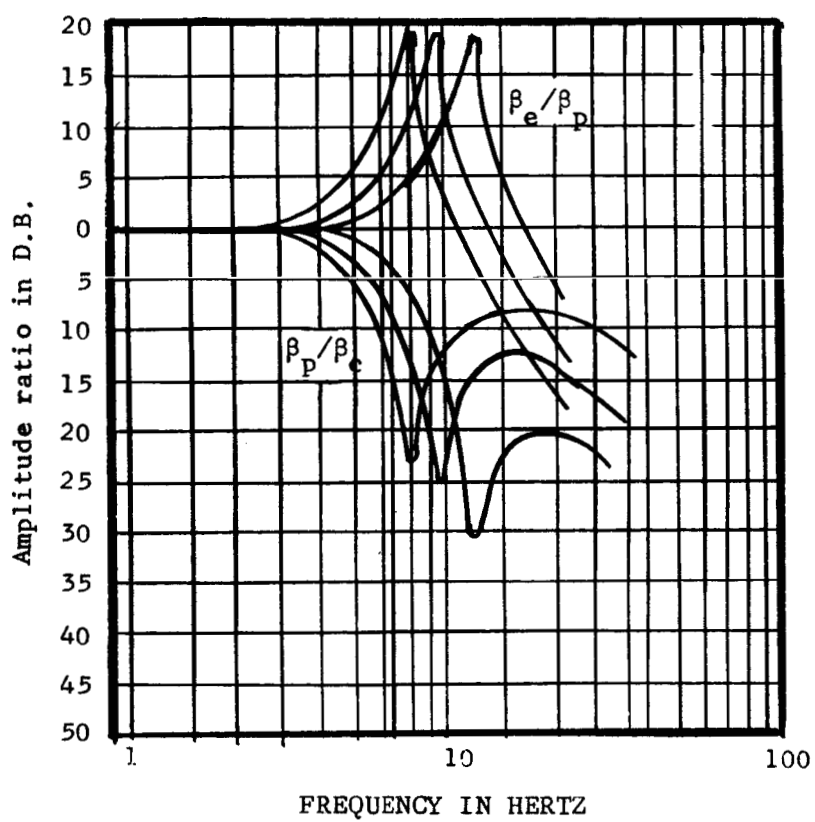


Figure 27. System response with load changes.

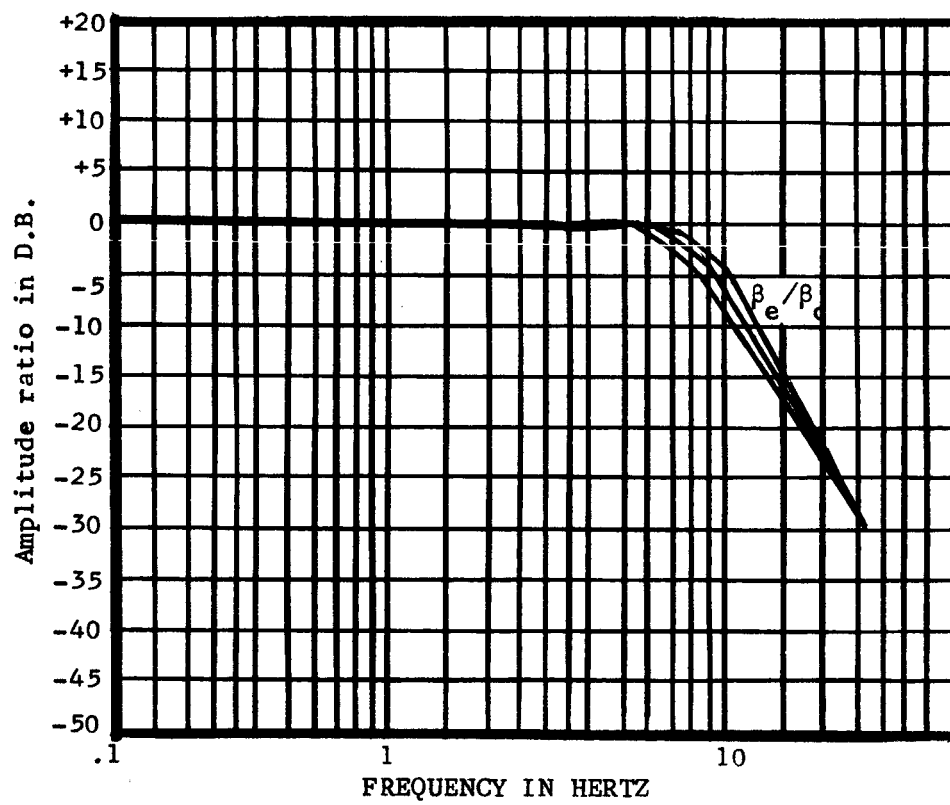


Figure 28. Overall system response.

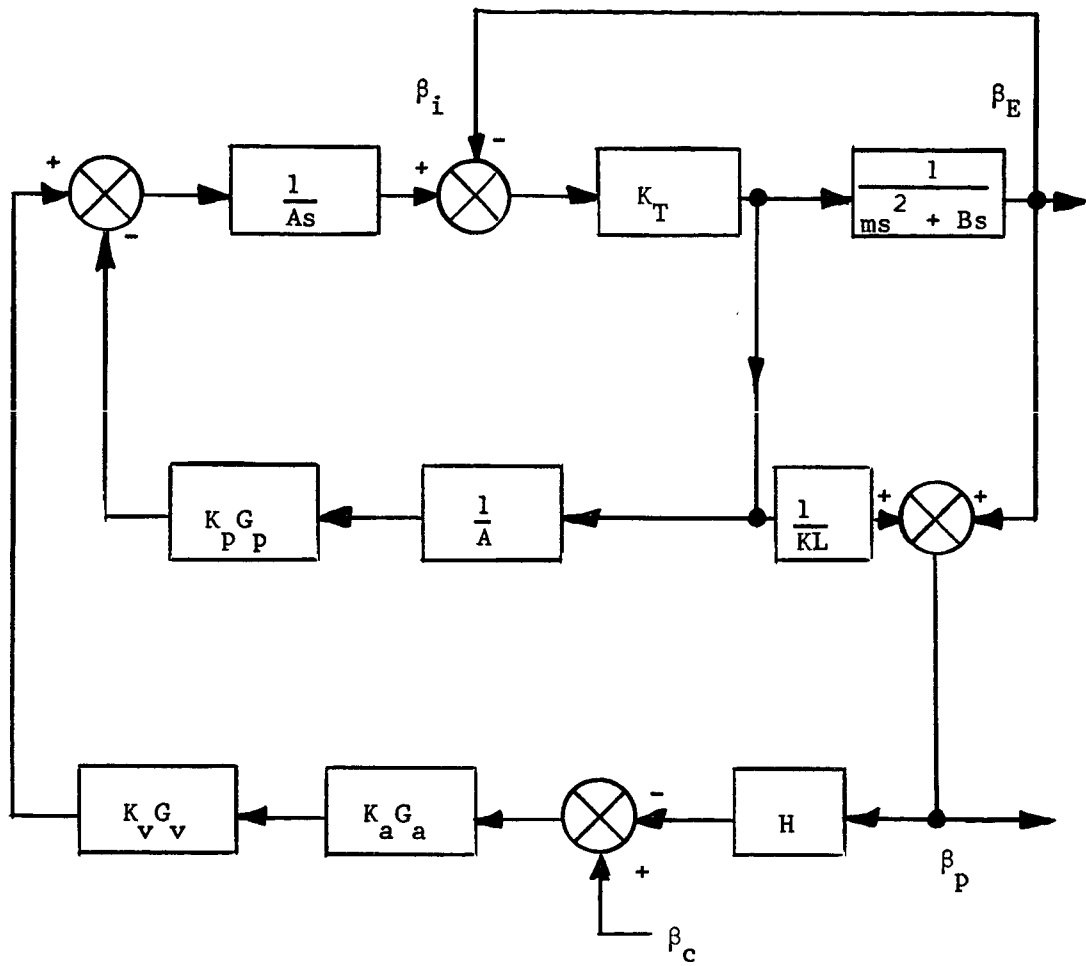


Figure 29. Block diagram for analog simulations.

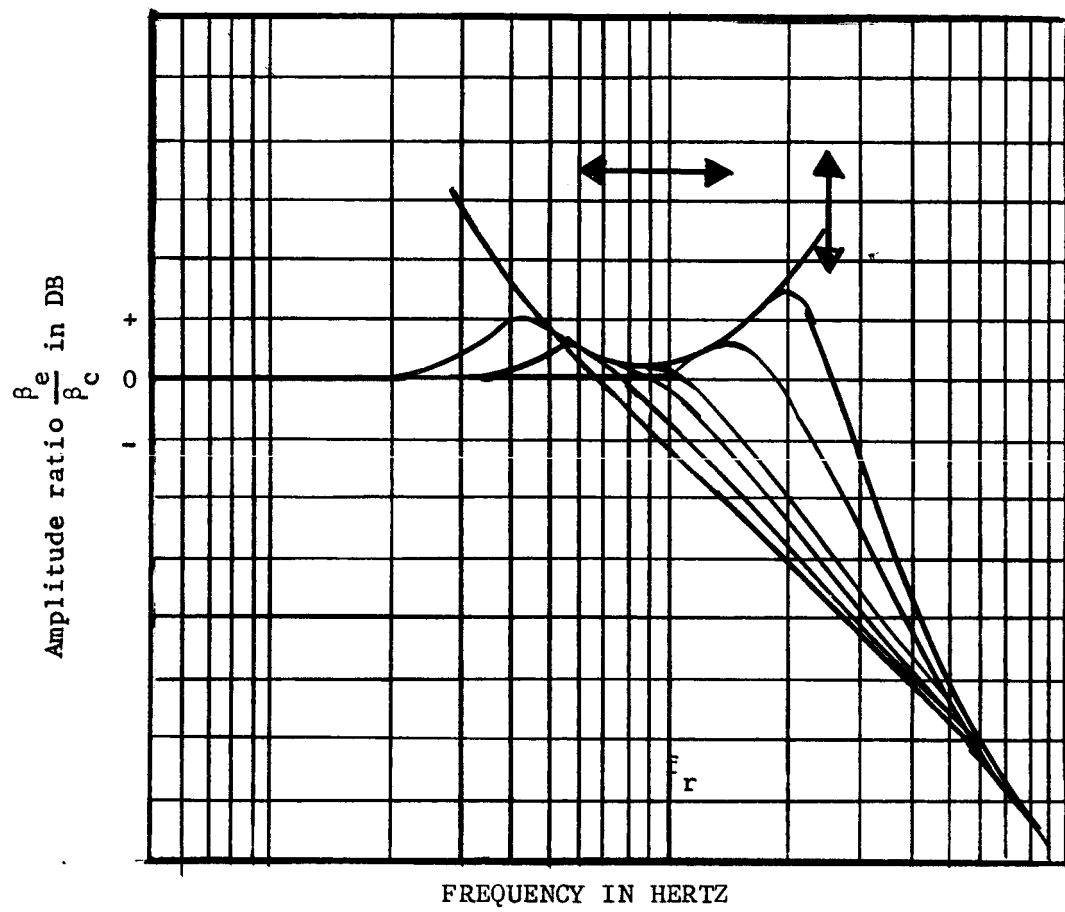


Figure 30. Response of system with pressure loop gain adjustment.

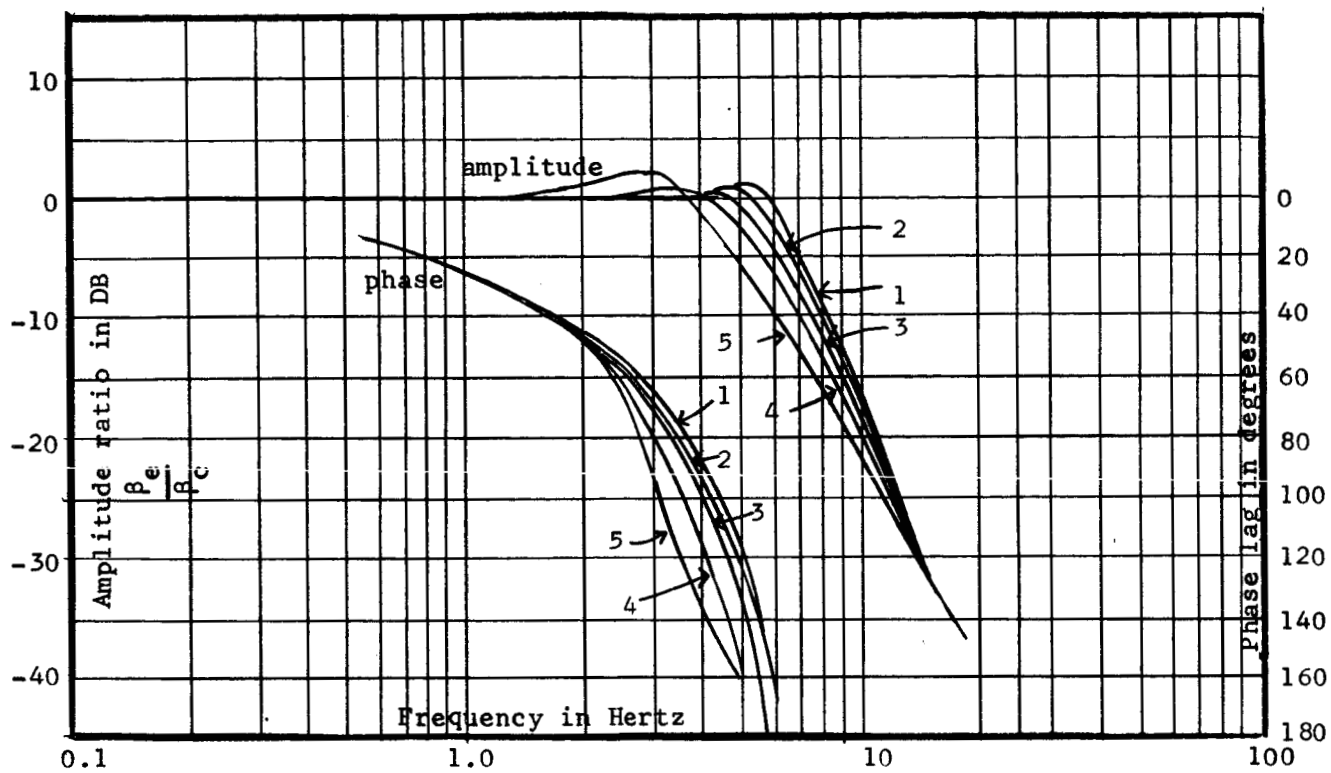


Figure 31. Analog runs of system.

The TVC system presented here will not solve all actuation problems. It does solve many and has much to offer for large mass gimbal systems. This dynamic shaping network is not the only way one can mechanize the required differential equations, however, it does give some latitude in choosing other components of the TVC system.

Although the equations for the servo-valve presented here are sufficient for design and sizing the system, more work should be done to isolate trouble spots. The individual blocks presented in Figure 7, page 18, should be evaluated mathematically to completely enable the design engineer to cope with any type of unexpected interface problem.

REFERENCES

LIST OF REFERENCES

1. Blackburn, J. F., Gerhard Reethof, and J. L. Shearer. Fluid Power Control. New York: The Technology Press of M.I.T. and John Wiley and Sons, Inc., 1960.
2. Lewis, E. E., and Hansjoerg Sterns. Design of Hydraulic Control Systems. New York: McGraw-Hill Book Company, Inc., 1962.
3. Truxal, John G. Control Engineers' Handbook. New York: McGraw-Hill Book Company, Inc., 1958.
4. Truxal, John G. Automatic Feedback Control Systems Synthesis. New York: McGraw-Hill Book Company, Inc., 1953.
5. Rouse, Hunter, and J. W. Howe. Basic Mechanics of Fluid. New York: John Wiley and Sons, Inc., 1953.
6. Thompson, Zack, and R. J. Alcott. "Apollo Booster Flight Control System," NASA TMX-53320, NASA Technical Memorandum, August, 1965.
7. Thompson, Zack. "The Linear Equations and Nonlinear Models for the Saturn V Vehicle Thrust Vector Control System," 12-ASTR-NFS-134-66, MSFC Memorandum, April, 1966.
8. Thompson, Zack. "Analysis of the Nonlinear Hydraulic Servoactuator for the S-IC Stage of Saturn V," R-ASTR-NFM-162-65, MSFC Memorandum, June, 1965.
9. Thompson, Zack. "The Linear Equations and Nonlinear Models for Saturn IB Thrust Vector Control System," R-ASTR-NFM-128-65, MSFC Memorandum, March, 1965.
10. Thompson, Zack, and Perry Davis. "Actuator Participation in a Bending Mode Identification System," The Society of Automotive Engineers Committee A-18 Aerospace Vehicle Flight Control System, Meeting No. 17, New Orleans, La., January, 1966.
11. Thompson, Zack, and Perry Davis. "A Servo Loop Used as a Traveling Match Filter in a Thrust Vector Control System," MSFC, Astrionics Laboratory paper, 1966.
12. Thompson, Zack, and James Lominick. "Servoactuator Mechanical Feedback Considerations," M-ASTR-N-441, MSFC Memorandum, August, 1963.

13. Thompson, Zack. "Saturn TVC Parameters," R-ASTR-NF-276-64, MSFC Memorandum, July, 1964.
14. Thompson, Zack. "Guidelines for Actuator Load Calculations," R-ASTR-NF-238-64, MSFC Memorandum, June, 1964.
15. Morse, Allen C. Electrohydraulic Servomechanisms. New York: McGraw-Hill Book Company, Inc., 1963.
16. Baltus, George T. "Application of Mechanical Feedback Servoactuators to Control Systems," The Society of Automotive Engineers A-6 Committee Meeting, New Orleans, La., March, 1966.
17. Kalange, M. A., and V. R. Neiland. "Saturn I Engine Gimbal and Thrust Vector Control Systems," The National Conference on Industrial Hydraulics, October, 1963.
18. Kalange, M. A., and R. J. Alcott. "Saturn V S-IC Stage Engine Gimbal Actuation System," S.A.E. Aerospace Fluid Power System and Equipment Conference, May, 1965.
19. Kalange, M. A., W. H. Pollock, and W. J. Thayer. "The Development of Servovalves with Improved Reliability for Space Vehicles," S.A.E. Committee A-6 Aerospace Fluid Power Techniques Conference, Boston, Mass., September, 1964.
20. Garnjost, K. D., and W. J. Thayer. "New Servovalves for Redundant Electrohydraulic Control," Joint Automatic Control Conference, Minneapolis, Minnesota, June, 1963.
21. Berger, J. B. "Application of Volterra Series Analysis to an Electrohydraulic Control Valve," Joint Automatic Control Conference, Stanford, California, June, 1964.
22. Weaver, C. H. "Preliminary Study of Engine Position Control," Auburn University, August, 1961.
23. Russell, D. W. "Study of Space Vehicle Engine Position Central Systems," Auburn Research Foundation, Inc., Technical Report, December, 1961.
24. Davis, P. W. "Equations Describing the Engine Position Control System for the Saturn S-1 Stage of the SA-5 Vehicle," M-ASTR-IN-63-7, MSFC Internal Note, March, 1963.
25. Thayer, W. J. "Design Considerations for Mechanical Feedback Servoactuators," Moog Servocontrols, Inc., Technical Report 104, April, 1964.

26. Thayer, W. J. "Transfer Functions for Moog Servovalves," Moog Servocontrols, Inc., Technical Bulletin 103, January, 1965.
27. Mack, J. "Preliminary Analysis of a SATURN Hydraulic Servo System," George C. Marshall Space Flight Center, Huntsville, Alabama, Memorandum dated August 25, 1961.
28. Thompson, Zack. "Empirical Response Equations for the Pershing Attitude Control Hydraulic Servo Systems," MTP-M-G&C-61-14, MSFC Technical Report, March, 1961.

APPENDICES

APPENDIX A

EXAMPLE

This example will demonstrate the mathematical relationships that have been derived. The block diagram as shown in Figure 32 has been reduced to its simplest form. The closed loop frequency response is shown in Figure 33.

$$K_a G_1 = \frac{9.09}{\left[\frac{S^2}{(300)^2} + \frac{2(0.7)S}{300} + 1 \right]}$$

$$K_v G_2 = \frac{0.53 \left[\frac{S}{18.86} + 1 \right]}{\left[\frac{S}{21.45} + 1 \right] \left[\frac{S}{377} + 1 \right]}$$

$$\frac{HG_3}{A} = \frac{2.82}{0.6} \left[\frac{1}{S} \right]$$

$$G_4 = \frac{\left[\frac{S^2}{(80.38)^2} + \frac{2(0.05)S}{80.38} + 1 \right]}{\left[\frac{S^2}{(70.57)^2} + \frac{2(0.416)S}{(70.57)} + 1 \right]}$$

$$G_5 = \frac{1}{\left[\frac{S^2}{(80.38)^2} + \frac{2(0.05)S}{80.38} + 1 \right]}$$

The open loop transfer function for this system is

$$F_o = \frac{22.64 \left[\frac{S}{18.86} + 1 \right] \left[\frac{S^2}{(80.38)^2} + \frac{2(0.05)S}{80.38} + 1 \right]}{S \left[\frac{S}{21.45} + 1 \right] \left[\frac{S}{377} + 1 \right] \left[\frac{S^2}{(300)^2} + \frac{2(0.7)S}{300} + 1 \right] \left[\frac{S^2}{(70.57)^2} + \frac{2(0.416)S}{70.57} + 1 \right]}$$

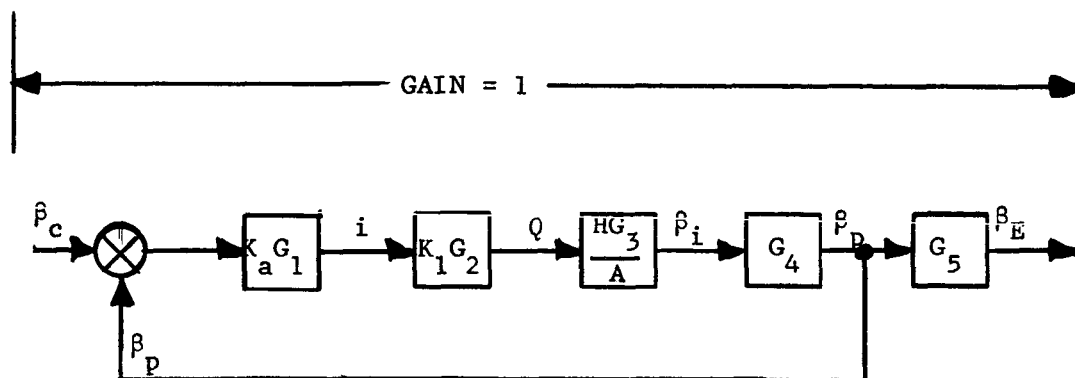


Figure 32. System block diagram.

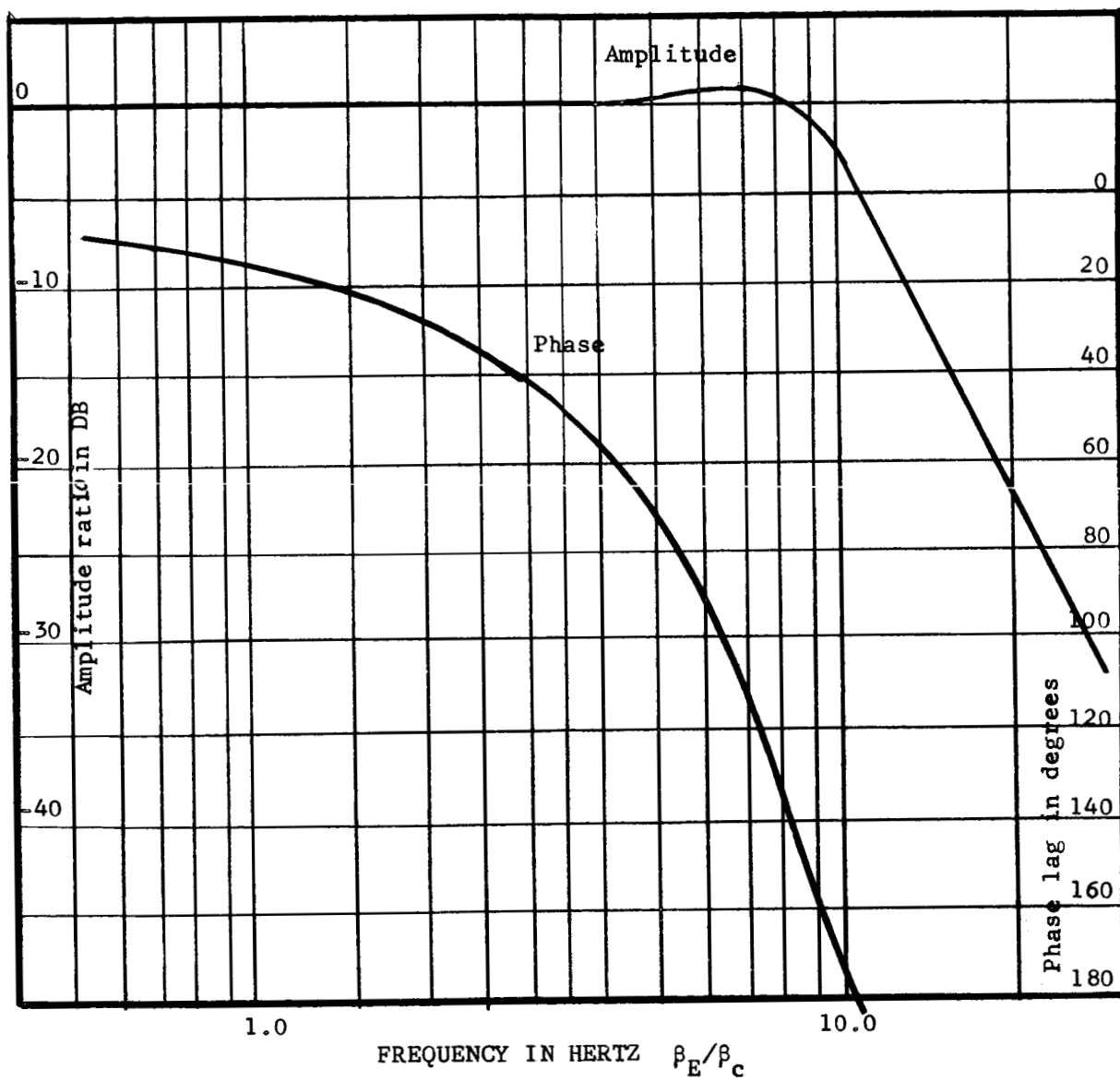


Figure 33. Engine frequency response.

A root locus plot of this equation, which reflects the versatility of the system as the open loop gain is varied, is shown in Figures 34 and 35.

After combining and simplifying the blocks in Figure 32, the two blocks in Figure 36 result. Where

$$G_6 = \frac{1}{\left[\frac{S}{16.5} + 1 \right] \left[\frac{S}{64.18} + 1 \right] \left[\frac{S}{338.9} + 1 \right]} \times \frac{\left[\frac{S}{18.86} + 1 \right] \left[\frac{S^2}{(80.28)^2} + \frac{2(0.05)S}{(80.38)} + 1 \right]}{\left[\frac{S^2}{(279.57)^2} + \frac{2(0.745)S}{279.57} + 1 \right] \left[\frac{S^2}{(54)^2} + \frac{2(0.377)S}{54} + 1 \right]}$$

and

$$G_5 = \frac{1}{\left[\frac{S^2}{(80.38)^2} + \frac{2(0.05)S}{80.38} + 1 \right]}$$

The final results of β_E/β_C are obtained by combining the two blocks in Figure 36 and are shown in Figure 37. Where

$$G_7 = \frac{1}{\left[\frac{S}{16.5} + 1 \right] \left[\frac{S}{64.18} + 1 \right] \left[\frac{S}{338.9} + 1 \right]} \times \frac{\left[\frac{S}{18.86} + 1 \right]}{\left[\frac{S^2}{(279.57)^2} + \frac{2(0.745)S}{279.57} + 1 \right] \left[\frac{S^2}{(54)^2} + \frac{2(0.377)S}{54} + 1 \right]}$$

The actual laboratory results of β_E/β_C and β_P/β_C are shown in Figure 33 and Figure 38, respectively.

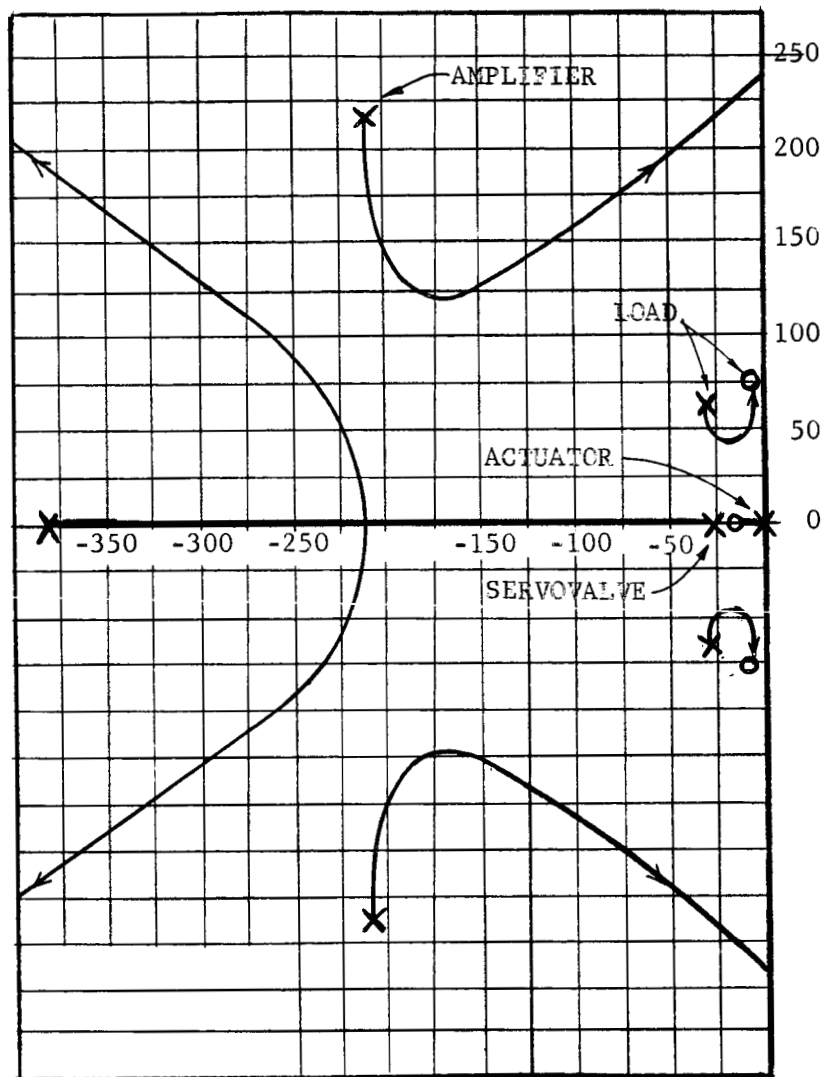


Figure 34. Root locus plot of open loop.

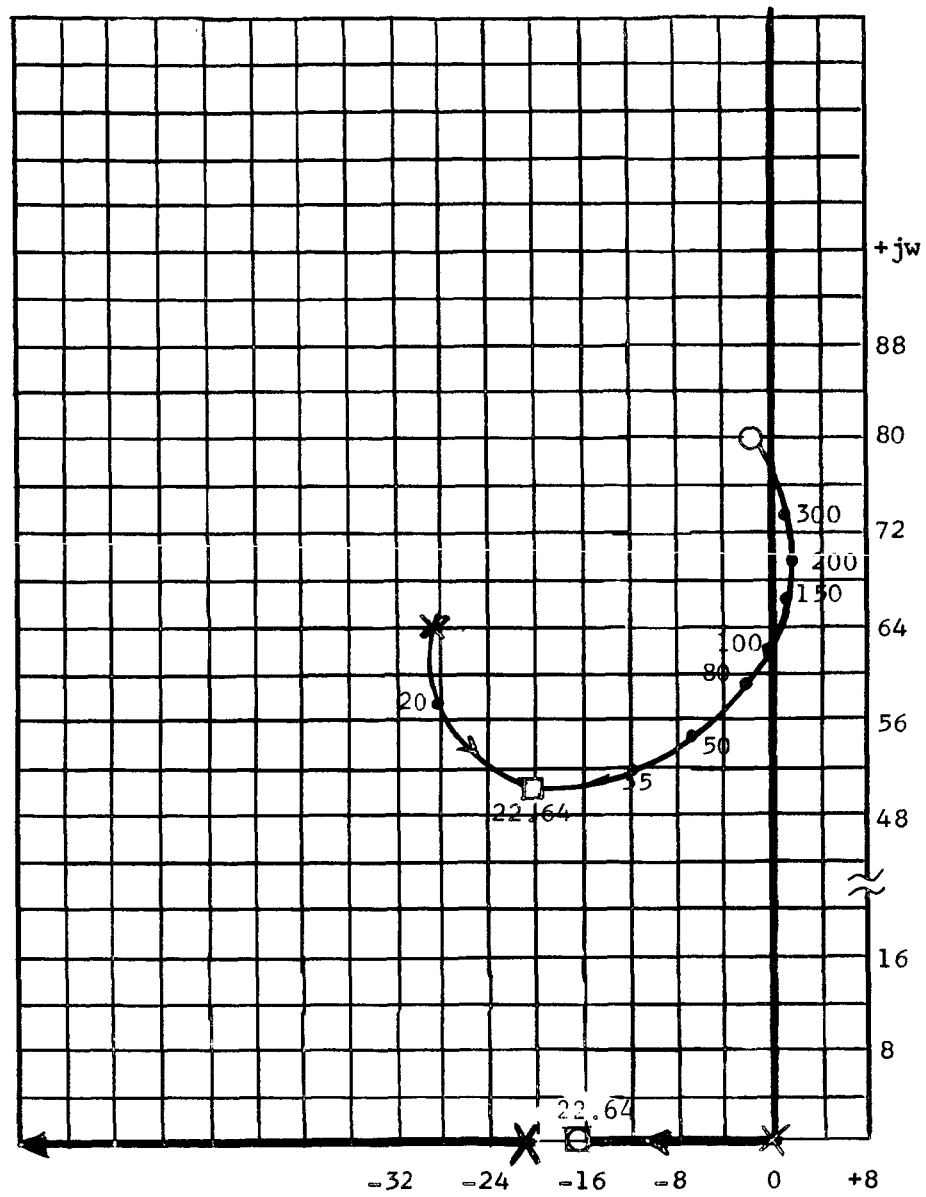


Figure 35. Expanded root locus plot of load bipole.

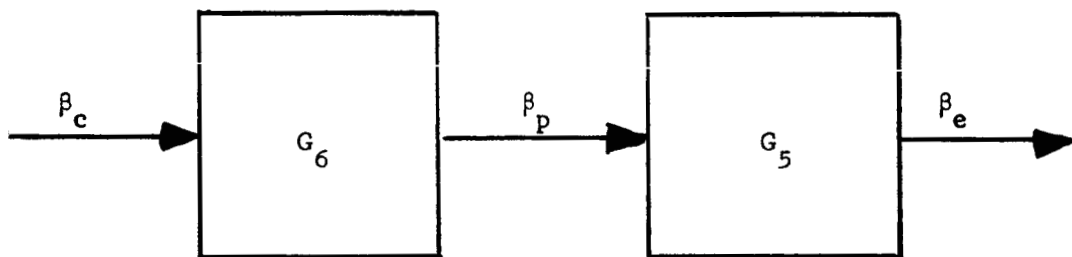


Figure 36. Double block diagram.

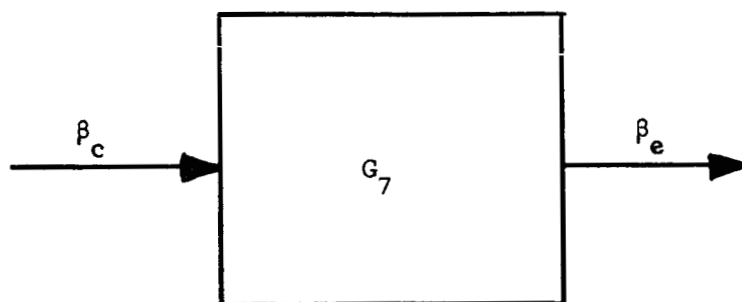


Figure 37. Single block diagram.

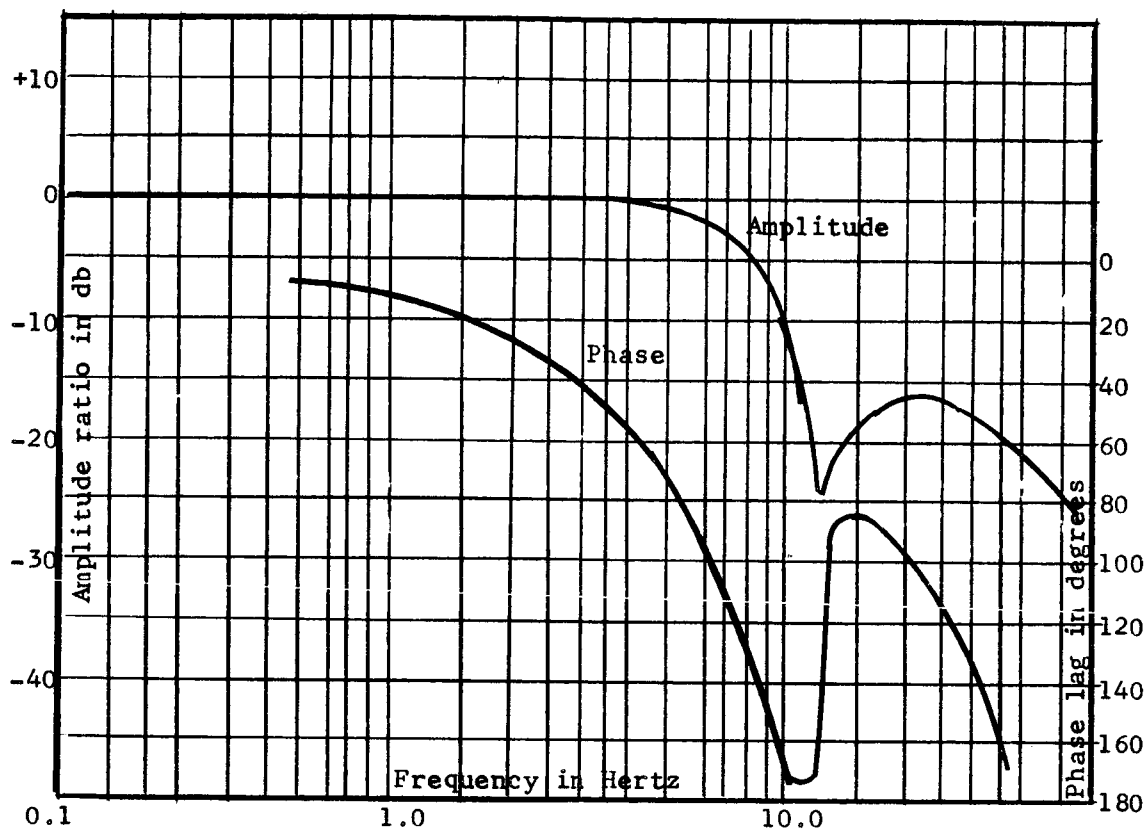


Figure 38. Actuator frequency response.

A root locus plot of the open loop gives the design engineer a complete picture of the closed loop root variations as a function of open loop gain. The poles and zeros of the reflected load transfer function β_p/β_i are the most critical parts of the root locus diagram. The expanded root locus plot of the reflected load is shown in Figure 35. One can see that if an open loop gain is picked large enough, the closed loop roots will be in the right half of the "S" plane, causing the TVC system to be unstable.

APPENDIX B

ASSUMPTIONS USED

The following assumptions are pertinent to the development of the TVC system mathematical model.

1. The hysteresis of the servo-valve and its effect on the system were neglected.
2. The compliances of the "O" rings were neglected.
3. The effect of leakage spools and actuator piston were assumed zero.
4. Blocked port parameters were not included.
5. The effects of lapping of valve (over-lapped on line, or under-lapped) were neglected.
6. The silting of valve was neglected.
7. Breakway forces and crushing power of valve were not analyzed.
8. Effects of contamination of hydraulic oil were omitted.
9. The amount of air and so forth, in hydraulic oil were not considered.
10. Air pockets in valve and hydraulic lines were neglected.
11. Flow through the valve was analyzed in one direction.
12. Size of wire and arrangements of coil in torque motor was neglected. (Reliability, etc.)
13. The type of metal for magnet and strength of magnets were not considered. (Assume one can get desired results.)

14. The type of metal for flapper and flexure tube was not considered.

15. The non-linearities in springs and feedback wires were omitted.

16. The losses in lines were assumed neglectable.

17. The hydraulic power supply was not analyzed. That is, it was assumed that one could get the desired pressures and flow rates required.